POLITÉCNICO DE LEIRIA

Polytechnic of Leiria
Superior School of Technology and Management
Department of Mechanical Engineering
Masters Degree in Automotive Engineering

CHASSIS DEVELOPMENT FOR A FORMULA STUDENT VEHICLE USING ADVANCED MATERIALS

RODRIGO FRANCISCO CEREJO DA SILVA

Leiria, September 2022

POLITÉCNICO DE LEIRIA

Polytechnic of Leiria
Superior School of Technology and Management
Department of Mechanical Engineering
Masters Degree in Automotive Engineering

CHASSIS DEVELOPMENT FOR A FORMULA STUDENT VEHICLE USING ADVANCED MATERIALS

STUDENT: RODRIGO FRANCISCO CEREJO DA SILVA
NUMBER: 2202280

Leiria, September 2022

ACKNOWLEDGMENTS

First of all, I would like to give a big thanks to all those who have helped me along this journey and my academic path.

To my dear family and friends who have helped me on various occasions with support and patience.

A really big thank you to all the members of my formula student team that were side by side developing the T22, it has been a huge learning experience journey, not only personally but with my colleagues that turned out into friends.

A big thanks to my colleagues on FST Lisboa, in particular to my friends André Carreira and Afonso Rainha who really helped me when i needed in clarifying this whole process by sharing their experience and knowledge.

And last but not least to my supervisors professor Sérgio Santos and Fernando Batista for all the support and guidance during this work.

RESUMO

O monocoque é um chassis, que representa o esqueleto de um veículo de competição, este é a maior estrutura presente no mesmo, onde todos os componentes são montados, tal como, ao qual, todos os esforços são transmitidos. Neste trabalho, esta estrutura é formada por painéis do tipo *sandwich*, estes são geralmente utilizados em áreas do desporto motorizado tal como em veículos de transporte onde é necessário uma elevada rigidez associada ao baixo peso, estes possuem duas faces exteriores em conjunto com um núcleo no meio.

O presente trabalho é realizado em volta de um chassis para um veículo do tipo *formula student* elétrico para a equipa FSIPLeiria, onde o objetivo é, através do dimensionamento dos vários painéis, de acordo com o regulamento da competição, e da análise de elementos finitos, obter uma estrutura rígida que cumpra com o regulamento e possa competir no futuro, seguidamente foi desenhada uma proposta de geometria do monocoque, para a análise das cargas dinâmicas, nos pontos de apoios da suspensão,e rigidez torsional de modo a optimizar a constituição da estrutura.

Foi possível de se concluir que o monocoque é uma estrutura superior a um chassis tubular convencional, constituído a partir de tubos de aço, em termos de rigidez em flexão e torsional, contudo estas vantagens vêm a um custo devido à complexidade durante todo o processo de desenvolvimento, tal como em produção como em custos monetários.

Palavras-chave: monocoque, FSAE, estruturas sandwich, materiais compósitos, elementos finitos

ABSTRACT

The monocoque is a chassis that represents the skeleton of a racing vehicle, this is the largest structure present within it, where all the components are mounted, as well as, all the loads are transmitted. In this work, this structure is formed by sandwich panels, which are generally used in motorsport areas, as well as in transportation vehicles where high rigidity is associated with low weight, these types of panels have two outer faces with a core in the middle.

The present work is done around a chassis for a formula student electric vehicle for the FSIPLeiria team, where the goal is, through the analysis of the various panels, according to the competition rules, and the finite element analysis, to obtain a rigid structure that complies with the regulations and will be able to compete in the future, then a project of the monocoque geometry was designed, for the analysis of the dynamic loads, at the suspension attachment points, and torsional stiffness in order to optimize the structure's composition.

It was possible to conclude that the monocoque is a superior structure to a conventional tubular chassis, made from steel tubes, in terms of bending and torsional stiffness, however, these advantages come at a cost due to the complexity during the whole development process, as well as in production and in monetary costs.

Keywords: monocoque, FSAE, sandwich structures, composite materials, finite elements

I N D E X

LIST OF FIGURES

LIST OF TABLES

LIST OF ACRONYMS

3D   Three Dimensional
3PBT   Three Point Bending Test

AIP   Anti-Intrusion Plate

BMS   Battery Management System

CAD   Computer Aided Design
CG   Center of Gravity
CNC   Computerized Numerical Control

FB   Front Bulkhead
FBHS   Front Bulkhead Bracing Supports
FDM   Fused Deposition Modeling
FEA   Finite Element Analysis
FS   Formula Student
FSAE   Formula SAE
FSAE TTC FSAE Tire Test Consortium

IA   Impact Attenuator
ICE   Internal Combustion Engine

KPA   Kingpin Angle
KPI   Kingpin Inclination

MDF   Medium-Density Fibreboard

NTNU   Norwegian University of Science and Technology

PET   Polyethylene Terephthalate

PS   Polystyrene

PSS   Perimeter Shear Strength

PST   Perimeter Shear Test

PU   Polyurethane

SAE   Society of Automotive Engineers

SES   Structural Equivalency Spreadsheet

SF   Safety Factor

SIS   Side Impact Structure

SLA   Stereolithography

TIRF   Tire Research Facility

WWFE   World Wide Failure Exercise

INTRODUCTION

1.1 MOTIVATION

Over the last few years, there have been many advancements in the area of composite materials and in the production of lighter yet stiffer and safer structures, capable of withstanding huge loads while weighing less than the more conventional materials like aluminum and steel. A great part of these advancements started in motorsport, eventually spreading to the automotive industry in order to save weight on the vehicles reducing fuel or electricity consumption[1].

The Formula Student competition is not different, here, students from various universities are challenged to design, and build themselves, a formula-type vehicle, with incredible dynamic capabilities, trough all the process that goes into making a car, students develop, not only hard but also soft skills that will help as future engineers.

The current work was done in collaboration with the Formula Student team from the Polytechnic of Leiria, FSIPLeiria, the team currently has three combustion vehicles and plans to expand its knowledge into making the first electric vehicle for the team as well as a full carbon fiber monocoque, both which have never been made before in this institution.

The monocoque is a chassis, that represents the skeleton of a racing vehicle, this is the largest structure present within it, where all the components are mounted, as well as, to which, all the loads are transmitted. As this is the main structure of a racing vehicle it is extremely important that it is well-designed and engineered, otherwise it can negatively affect the dynamic performance of the car as well as the safety of the driver, if the damage spreads through all the structure.

The theme for this project was selected, not only due to being an area of interest of mine but also to help my team´s progress in the development of a racing car to compete in one of the best motorsport competitions.

1.2 OBJECTIVES

The main objective of the current project is to design and develop a full carbon fiber monocoque from scratch.

Through the use of the classic theory of laminates and finite elements software, different simulations with different laminate configurations were made, for each panel, in order to find a suitable laminate, that is in compliance with the rules.

In addition, a design for the monocoque was made using Computer Aided Design software, in this case, Solidworks, in order to perform a study around the suspension loads applied on the monocoque outer shell, with the purpose of further improving the performance its geometry.

1.3 THESIS OUTLINE

The present thesis is divided into five different chapters:

- Chapter 1: Define the motivation that leads the author to choose the theme as well as the objectives for the current project.

- Chapter 2: A brief approach to the theory of composite materials, the types of materials, failure criteria, and a rough introduction to fatigue in composites, as well as carbon fiber sandwich panels and a background to the monocoque structures. Then, some concepts around torsional stiffness and vehicle dynamics as how the suspension loads were calculated, in the different arms.

- Chapter 3: Initial considerations that went into making the monocoque design and development through the clarification of the rules from the FSAE regulation, as some materials that are available for the study. The finite element analysis of the different sandwich panels, as well as the monocoque suspension loads in the geometry itself in order to optimize the monocoque structure and design, is also made a comparison between a conventional tubular space frame and a monocoque chassis.

- Chapter 4: Clarifies the manufacturing method that could be used for the manufacturing process of the monocoque, with the molds that are required, as well as the steps needed to be taken, to ensure that the monocoque structure is of good physical and structural quality.

- Chapter 5: Conclusion to the developed work, in the project, and some proposals for future works to improve the analysis method in the simulation and validation process as the design of the structure taking more variables into account like the pedal box and steering column attachments.

BACKGROUND

2.1 COMPOSITE MATERIALS

Materials can be divided into four different categories, metals, polymers, ceramics, and composites. The word composite means that two or more materials are combined on a macroscopic scale to create a new material, one of the many advantages of using composite-like materials is that if they are well developed, they will inherit the properties of both materials, that in most cases will mean that they will be stiffer with better strength, wear resistance, etc... Most made composite materials are composed of two materials (figure 1): a reinforcement material called fiber and a base material called the matrix material.

All the composite materials are generally arranged in three different groups [2]: the fibrous composites, which consist of the fibers being from one type of material and the matrix of another, the particle composites, which are formed by macro materials of one material and the matrix of another, in this type of composite either the fiber or the matrix can be metallic or non-metallic, and the laminated or structural composites, which each layer is made out of different materials, including composites of the first two types presented.

In composite materials [2], the strength and the stiffness come from the fiber, the shorter fibers are often called whiskers that present better stiffness and strength properties than long fibers. The matrix is responsible to keep the fibers together, while also acting as a load transfer to dissipate the loads through all the fibers and protect them from being in contact with the environment that surrounds them, protecting them from radiation, humidity, etc... The matrix, being an isotropic material, has almost the same properties as in bulk form, whereas the fibers, being an orthotropic material, have directionally dependent properties.
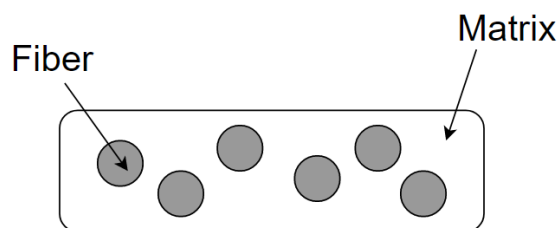
Figure 1: Basic composition of a composite material

2.1.1 *Isotropic Materials*

Unlike the fibers, the matrix is commonly made out of isotropic materials as previously mentioned, this means that the mechanical and thermal properties of the material are the same along the three different axes, this means that whatever direction the force is applied in the deformation will be the same.

The stress-strain relation [3] for an isotropic material takes the form of the equation 1.

$$
\begin{Bmatrix} \sigma_1 \\ \sigma_2 \\ \sigma_3 \\ \sigma_4 \\ \sigma_5 \\ \sigma_6 \end{Bmatrix} = \Lambda \begin{bmatrix} 1-\nu & \nu & \nu & 0 & 0 & 0 \\ \nu & 1-\nu & \nu & 0 & 0 & 0 \\ \nu & \nu & 1-\nu & 0 & 0 & 0 \\ 0 & 0 & 0 & \frac{1}{2}(1-2\nu) & 0 & 0 \\ 0 & 0 & 0 & 0 & \frac{1}{2}(1-2\nu) & 0 \\ 0 & 0 & 0 & 0 & 0 & \frac{1}{2}(1-2\nu) \end{bmatrix} \begin{Bmatrix} \varepsilon_1 \\ \varepsilon_2 \\ \varepsilon_3 \\ \varepsilon_4 \\ \varepsilon_5 \\ \varepsilon_6 \end{Bmatrix} \tag{1}
$$

Where $E_1 = E_2 = E_3 = E, G_{12} = G_{13} = G_{23} = G$, $\nu_{12} = \nu_{13} = \nu_{23} = \nu$, and $\Lambda = E/(1+\nu)(1-2\nu)$.

2.1.2 *Orthotropic Materials*

As previously mentioned, the materials used in the fiber are commonly orthotropic, this means that the mechanical and thermal properties of the material are different along the three different axes.

The strain-stress relation [3] for an orthotropic material takes the form of the equation 2.

$$
\begin{Bmatrix} \varepsilon_1 \\ \varepsilon_2 \\ \varepsilon_3 \\ \varepsilon_4 \\ \varepsilon_5 \\ \varepsilon_6 \end{Bmatrix} = \begin{bmatrix} \frac{1}{E_1} & -\frac{\nu_{21}}{E_2} & -\frac{\nu_{31}}{E_3} & 0 & 0 & 0 \\ -\frac{\nu_{12}}{E_1} & \frac{1}{E_2} & -\frac{\nu_{32}}{E_3} & 0 & 0 & 0 \\ -\frac{\nu_{13}}{E_1} & -\frac{\nu_{23}}{E_2} & \frac{1}{E_3} & 0 & 0 & 0 \\ 0 & 0 & 0 & \frac{1}{G_{23}} & 0 & 0 \\ 0 & 0 & 0 & 0 & \frac{1}{G_{13}} & 0 \\ 0 & 0 & 0 & 0 & 0 & \frac{1}{G_{12}} \end{bmatrix} \begin{Bmatrix} \sigma_1 \\ \sigma_2 \\ \sigma_3 \\ \sigma_4 \\ \sigma_5 \\ \sigma_6 \end{Bmatrix} \tag{2}
$$

Where the E_1, E_2, E_3 are Young´s Modulus in 1, 2, and 3 in the main directions, respectively, ν_{ij} is Poisson´s Ratio, defined as the ratio of the transverse strain (jth direction) and the axial strain (ith direction), and G_{12}, G_{13}, G_{23} are shear modulus in the 1-2, 1-3 and 2-3 respectively.

2.1.3 *Laminae and Laminates*

A typical sheet of composite material is commonly referred to as a lamina or ply [2], a fiber-reinforced lamina consists of several fibers embedded in a matrix. These fibers can be continuous or discontinuous, woven, unidirectional, bi-directional, or randomly distributed (figure 2). Unidirectional fiber-reinforced laminae exhibit better mechanical properties in the direction zero of the fiber, i.e. the direction where all the fibers are lay-ed in, this means in this direction the fiber offers the highest strength and modulus. Poor bonding between the fibers and the matrix will always result in failures like fiber pull-out, and fiber buckling due to poor transverse properties of the fiber reinforced composite. The composites reinforced with discontinuous fibers always have lower strength and modulus compared to the continuous fibers.
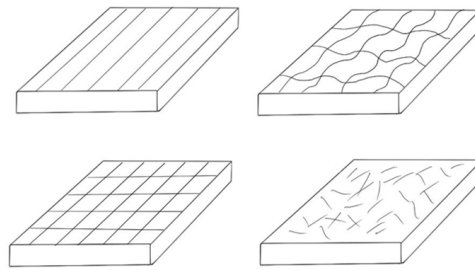
Figure 2: Different type of fibers

A laminate is a collection of different plies stacked together in order to achieve higher strength, stiffness, and desired thickness, per example it is possible to stack up different plies with different orientations from each other in order to have a higher strength and stiffness in various directions, this method is also known as lamination scheme or stacking sequence shown in the figure 3.

As a common rule, the material used in the matrix is generally also used to bond the different layers in the laminate. If a laminate has plies oriented at 30 or 45 degrees, the laminate will have a greater resistance to shear loads. The way that a laminate is designed will also influence the way that it flexes when a force is applied to it.
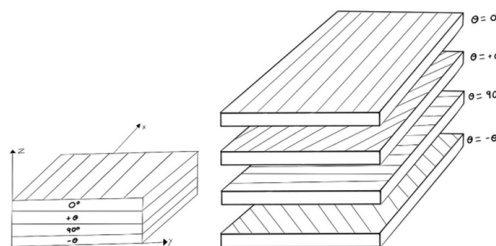
Figure 3: Fiber stacking - laminate

Despite all the great advantages of the fiber-reinforced composite materials, there are also disadvantages associated with the use of these types of materials that need to be addressed, for example, due to a mismatch of the material properties between the various layers of the shear forces, especially on the edges of the laminate, can result in the process of delamination, i.e. when the shear forces exceed the shear stress of the laminate and the various layers slip on each other, breaking the bond between them resulting in the failure of the laminate.

Failures may also occur during the production of the laminate due to material defects and human error such as void areas where there is no matrix material between the fibers, wrong fiber orientation, the fiber being damaged at one point or even having a variation of the thickness. For this and many more reasons it is important in the process of developing and produce a part or structure to take these defects into account in order to prevent them, as well as adopting production methods that minimize the probability of failure.

2.1.4 *Failure Criteria*

For the structural analysis of every composite material, it is important to define which failure criteria will be used. A brief research was carried out regarding this topic, there is an available study [4] that is communally known as the World-Wide Failure Exercise or WWFE, led by **Adbul-Salam** in which, through the use of several specimens sent to several research facilities. In this research, it was possible to define the failure criteria with the greatest predictability, that is, those that were better able in predicting the failure of the various test pieces when they are under the effect of one or several types of loads.

When going through this document, it is possible to conclude that the criteria that best fits this analysis are the Tsai-Hill criteria as can be seen in the figure 4, these criteria among the others, are the most accurate predicting (where the value closer to 1 is the most realistic) the initial failure of the composite as well as the delamination and the final failure, that is rupture. To complement this analysis, the maximum stress and strain criteria will also be used.
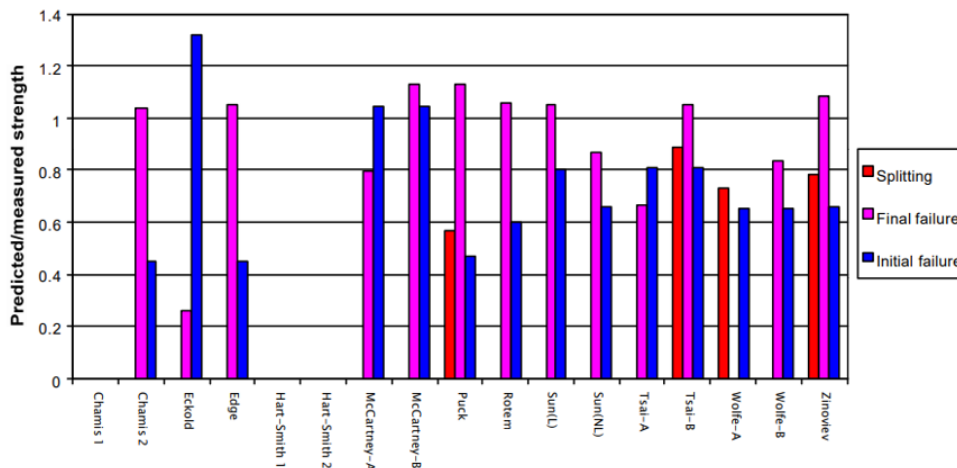
Figure 4: World-Wide Failure Exercise results, adapted from [4]

2.1.4.1 *Maximum Stress: Failure Criterion*

This theory was first introduced in 1920 by **Jenkins** [5] as an extension of the maximum normal stress theory for isotropic materials, the failure of the composite occurs as soon as the stress field no longer satisfies the following relations:

$$\sigma_{1rc} < \sigma_1 < \sigma_{1rt}, \quad -\sigma_{4r} < \sigma_4 < \sigma_{4r}$$
$$\sigma_{2rc} < \sigma_2 < \sigma_{2rt}, \quad -\sigma_{5r} < \sigma_5 < \sigma_{5r} \tag{3}$$
$$\sigma_{3rc} < \sigma_3 < \sigma_{3rt}, \quad -\sigma_{6r} < \sigma_6 < \sigma_{6r}$$

Where $\sigma_{irt}(i = 1,2,3)$ represents the failure stresses in tension, $\sigma_{irc}(i = 1,2,3)$ the failure stresses in compression, and $\sigma_{ir}(i = 4,5,6)$ the shear failures stresses. In these expressions the failure stresses in tension are positive and the compression ones are negative.

The loading coefficient $F_{i\sigma}$ is associated with the stress state leading to failure, it is convenient to introduce this coefficient for each expression when the stress state of the composite is expressed as a function of a single parameter which depends on external loads [3].

This stress state can be defined by:

$$\sigma_i' = F_{i\sigma}\sigma_i, \tag{4}$$

leads to the loading coefficients:

$$F_{i\sigma} = \frac{\sigma_{irc}}{\sigma_i} \quad or \quad F_{i\sigma} = \frac{\sigma_{irt}}{\sigma_i} \quad (i = 1,2,3), \tag{5}$$

Whether the normal stresses are in tension and shear (positive) or compression (negative) and:

$$F_{i\sigma} = -\frac{\sigma_{ir}}{\sigma_i} \quad or \quad F_{i\sigma} = \frac{\sigma_{ir}}{\sigma_i} \quad (i = 4,5,6), \tag{6}$$

Whether the shear stresses are positive or negative (depending on the direction).

The failure of the composite occurs for the smallest value of the loading coefficient $F_{i\sigma}$, calculated above, according to the failure mode given by the index i. For $i = 1,2$ or 3 X_1, X_2 or X_3, whereas for $i = 4,5$ or 6 (X_2,X_3), (X_3,X_1) or (X_1,X_2) respectively.

2.1.4.2 *Maximum Strain: Failure Criterion*

In 1967, **Waddoups** [5] proposed the maximum strain theory for the orthotropic laminae as an extension of the maximum normal strain theory (or Saint Venant´s Theory) for isotropic materials. This criterion predicts the failure when any principal material axis strain exceeds the corresponding ultimate strain of the material, this means when the strain field no longer satisfies the following relations:

$$\varepsilon_{1rc} < \varepsilon_1 < \varepsilon_{1rt}, \quad -\varepsilon_{4r} < \varepsilon_4 < \varepsilon_{4r}$$

$$\varepsilon_{2rc} < \varepsilon_2 < \varepsilon_{2rt}, \quad -\varepsilon_{5r} < \varepsilon_5 < \varepsilon_{5r} \tag{7}$$

$$\varepsilon_{3rc} < \varepsilon_3 < \varepsilon_{3rt}, \quad -\varepsilon_{6r} < \varepsilon_6 < \varepsilon_{6r}$$

Where $\varepsilon_{irt}(i = 1,2,3)$ represents the failure strains in tension, $\varepsilon_{irc}(i = 1,2,3)$ the failure strains in compression, and $\varepsilon_{ir}(i = 4,5,6)$ the shear failures strains. In these expressions the failure strains in tension are positive and the compression ones are negative.

Just as in the maximum stress theory, if the strain state only depends on one parameter we can define for each expression the maximum strain coefficient $F_{i\varepsilon}$ which is associated with the strain state leading to failure [3].

The strain state:

$$\varepsilon_i' = F_{i\varepsilon}\varepsilon_i, \tag{8}$$

gives the loading coefficients:

$$F_{i\varepsilon} = \frac{\varepsilon_{irt}}{\varepsilon_i} \quad or \quad Fi_\varepsilon = \frac{\varepsilon_{irc}}{\varepsilon_i} \quad (i = 1,2,3), \tag{9}$$

$$F_{i\varepsilon} = \frac{\varepsilon_{ir}}{\varepsilon_i} \quad or \quad F_{i\varepsilon} = -\frac{\varepsilon_{ir}}{\varepsilon_i} \quad (i = 4,5,6), \tag{10}$$

just like the maximum stress theory, the same remarks concerning the signs of the sign convention and the failure modes.

2.1.4.3 *Tsai-Hill: Failure Criteria*

The most important failure criteria are quadratic, which means that they are expressed as a function of the stresses in the form of 2nd-degree polynomials. This criterion comes from Hill´s criteria of plastic yielding of metals, Hill em 1948 [6], took into consideration the Von-Misses yield criterion developed around the isotropic metals, to describe the anisotropy resulting from strain hardening.

For an orthotropic material [3] the Tsai-Hill criteria is written as:

$$A(\sigma_1 - \sigma_2)^2 + B(\sigma_2 - \sigma_3)^2 + C(\sigma_3 - \sigma_1)^2 + D\sigma_4^2 + E\sigma_5^2 + F\sigma_6^2 < 1 \tag{11}$$

The six constants A, B, C, D, E and F are determined from six independent loading cases.

For failure by extension in the X_1 direction then X_2 and finally X_3, we obtain the three following expressions:

$$A + C = \frac{1}{\sigma_{1r}^2}, \quad A + B = \frac{1}{\sigma_{2r}^2}, \quad B + C = \frac{1}{\sigma_{3r}^2}, \tag{12}$$

Whereas failure by shear in the plane (X_2, X_3) and then (X_3, X_1) and finally (X_1, X_2), we obtain the three missing expressions:

$$D = \frac{1}{\sigma_{4r}^2}, \quad E = \frac{1}{\sigma_{5r}^2}, \quad F = \frac{1}{\sigma_{6r}^2}. \tag{13}$$

By identification of the polynomial, we can obtain the following non-zero coefficients $F_i j$:

$$
\begin{aligned}
F_{11} &= \frac{1}{\sigma_{1r}^2}, \qquad F_{22} = \frac{1}{\sigma_{2r}^2}, \qquad F_{33} = \frac{1}{\sigma_{3r}^2}, \\
F_{44} &= \frac{1}{\sigma_{4r}^2}, \qquad F_{55} = \frac{1}{\sigma_{5r}^2}, \qquad F_{66} = \frac{1}{\sigma_{6r}^2}, \\
F_{12} &= -\frac{1}{2}\left(\frac{1}{\sigma_{1r}^2} + \frac{1}{\sigma_{2r}^2} - \frac{1}{\sigma_{3r}^2}\right), \\
F_{23} &= -\frac{1}{2}\left(\frac{1}{\sigma_{2r}^2} + \frac{1}{\sigma_{3r}^2} - \frac{1}{\sigma_{1r}^2}\right), \\
F_{31} &= -\frac{1}{2}\left(\frac{1}{\sigma_{3r}^2} + \frac{1}{\sigma_{1r}^2} - \frac{1}{\sigma_{2r}^2}\right).
\end{aligned}
\tag{14}
$$

In the expressions above the failure stresses, σ_{ir} $(i = 1,2,3)$ will be take equal to the tensile failure stress σ_{irt} for σ_i for positive, and in compression σ_{irc} for σ_i for negative.

The failure of the composite will occur when the stress field is greater than 1, i.e. it no longer satisfies the expression:

$$F_{11}\sigma_1^2 + F_{22}\sigma_2^2 + F_{33}\sigma_3^2 + 2F_{23}\sigma_2\sigma_3 + 2F_{31}\sigma_3\sigma_1 + 2F_{12}\sigma_1\sigma_2 + F_{44}\sigma_4^2 + F_{55}\sigma_5^2 + F_{66}\sigma_6^2 < 1. \tag{15}$$

2.1.5 *Fatigue in Fiber Composites*

Unlike metals, [7] composite materials are normally anisotropic, this means the properties of the material will change in all directions along the object itself, they accumulate damage rather than in a localized fashion, and most of the time the failure does not occur by the propagation of a macroscopic crack. The microstructural mechanisms of damage accumulation, including fiber breakage, matrix cracking, debonding, delamination, etc... occurs sometimes, independently or interactively, and the predominance of one or the other may be strongly affected by some variables like the composition of the materials, the testing environment, etc...

At low levels of stress, most of the composites sustain damage, this damage is distributed through the stress area, reducing the stiffness of that general area although it does not always result in a lower strength. This reduction of strength can be referred to as the composite starting to wear out. Later in life, the amount of damage that the composite has accumulated in some of its regions will fall into values of maximum stress in the fatigue cycle and will result in failure as it can be shown in the figure 5.
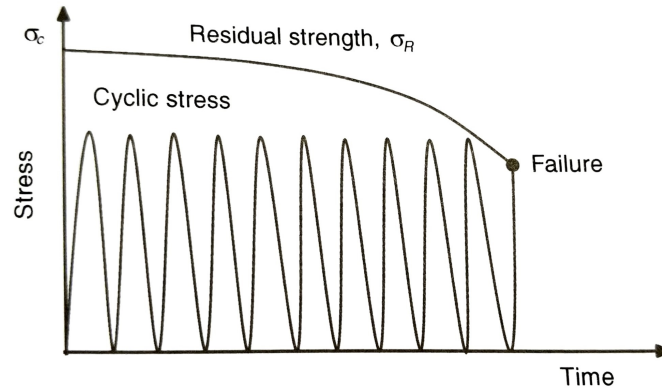
Figure 5: Degradation of composite strength caused by wear-out of composite material, adapted from [7]

2.2 SANDWICH COMPOSITES STRUCTURES

Sandwich structures consist of two laminated shells of high stiffness and strength in the exterior and in the middle, a core between the two shells (figure 6), these components combined together take advantage of both material properties as well as giving a structural advantage to the structure, these type of structures can withstand great forces just like a conventional solid material with the advantage of being several times lighter, the use of the core in the middle increases the cross section area giving it greater resistance to bending forces and torsional stiffness providing a higher weight to stiffness ratio.
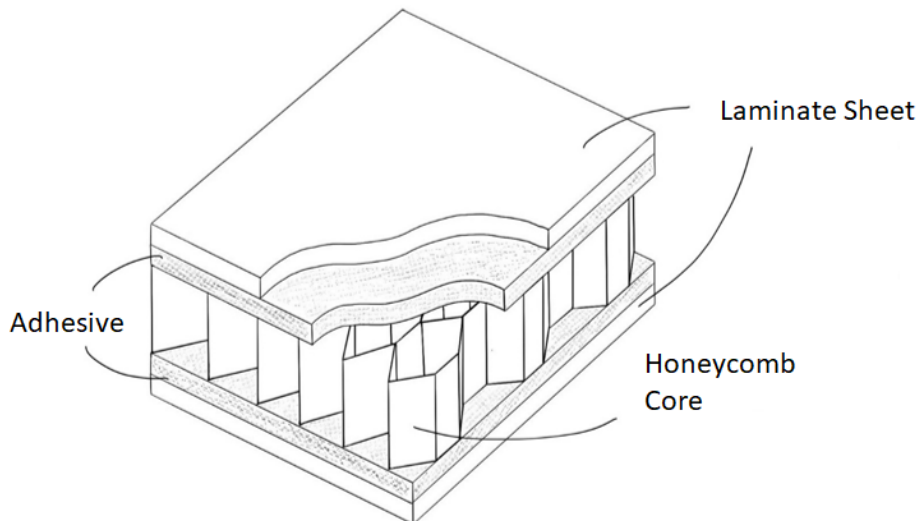
Figure 6: Sandwich laminate panel

These structures are commonly found in multiple engineering fields like automotive, aerospace, marine, and others, due to their superior capabilities and mechanical properties.

These types of structures can be made out of a wide range of materials in the laminate sheets, these can be commonly made out of glass fiber, carbon fiber, or aluminum sheets, while in the core is generally used aluminum honeycomb or Nomex and foam cores.

2.3 MONOCOQUE STRUCTURE

The monocoque, from the french "single" (mono) and "hull" (coque), is a structural technique in which the stresses and loads are applied to an outer shell of a given material instead of a set of tubes as in the case of a tubular chassis, besides being a structural component, it has a great aerodynamic role. One of the great advantages of using this type of structure is a great ratio of structural stiffness and weight, however, it contains a big weakness being its structural instability, that is, having a great probability of failure if not well designed, developed, and manufactured. One of the solutions to prevent it from happening, while for reinforcing the structure is the use of internal structures, like stringers or bulkhead cross frames acting as a skeleton of the monocoque figure 7, although these internal structures add weight they are necessary to maintain its stiffness. Most of the structure of the monocoque is made out of sandwich panels to maintain its structural stiffness and strength so it's compliant with the rules.

Figure 7: Internal structures inside the monocoque, adapted from[8]

Taking as an example the highest level of competition, McLaren was the first team to introduce this structural technique into the motorsport world, with the production of the first carbon-fiber reinforced composite monocoque in just 1981 (figure 8). From this point on, this technique became widely used by all the other teams as well as in various formula and motorsport competitions.

In the formula student (FS) competition, this structural technique has been adopted by several teams due to its excellent properties, however, this technique also comes with high price costs for the materials as well as requiring extensive knowledge in the area of composites materials compared to the use of a space frame chassis that uses conventional steel tubes.

Figure 8: McLaren MP4-1 monocoque, adapted from[9]

When choosing what type of monocoque to use, there are several concepts available depending on the goal of the team, as well as the type of powertrain that will be used in the formula. In cases where the power comes from an internal combustion engine (ICE), its more common to use a hybrid monocoque (figure 9 a)) which means that, from the main hoop forward it´s all a single monocoque whereas in the back is a tubular structure to accommodate the engine, this type of structure helps in the heat dissipation from the ICE, for the case in study, the formula is intended to be an electric vehicle where the power comes from two electric motors in the rear, a full monocoque, like the one in the figure 9 b) is a better option, due to the fact that the electric motors, inverters and the accumulator do not produce as much as the ICE on a combustion vehicle and provides greater stiffness and torsional stiffness.

a)   b)
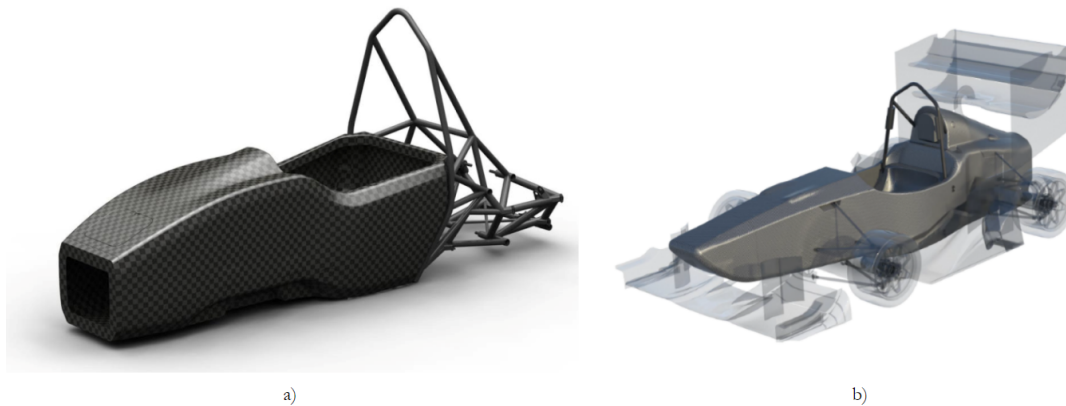
Figure 9: FSAE types of monocoque, a) Hybrid monocoque, b) Full monocoque, adapted from [10] and [11] respectively

2.4 TORSIONAL STIFFNESS

Since the main topic of this work is the development of a chassis for an FS vehicle, it is important to mention the torsional stiffness of a chassis.

According to **Milliken** [12], Stiffness is the resistance a body offers to a bending or flexing momentum, and torsional resistance refers to the resistance of a twisting motion.

It can be assumed that the behavior of a chassis resembles a large spring, which connects the front suspension to the rear one, a lack of stiffness, i.e. if it has high flexibility it can compromise the lateral load transfer during cornering and add very complex variables to an already complex system that is the suspension of the vehicle. Predictable handling can be achieved in a better way when the chassis is stiff enough for this variable to be ignored in a way, which simplifies the calculations present in the first part of the next section.

Trough the equation 16 to calculate the angular deformation and the equation 17 to calculate the torsional stiffness itself (K_T) (adapted from [13]), is possible to calculate the torsional stiffness of the chassis, the variables are specified in the figure 10. It is essential to mention that the formula, for the angular deformation (16), is only valid when a maximum displacement is a low value, due to the fact that its an approximation to a straight line when in fact, the trajectory is an arc when a force is applied.

$$\theta = \frac{\delta}{L} \tag{16}$$

$$K_t = \frac{2 * F * L}{\theta} \tag{17}$$
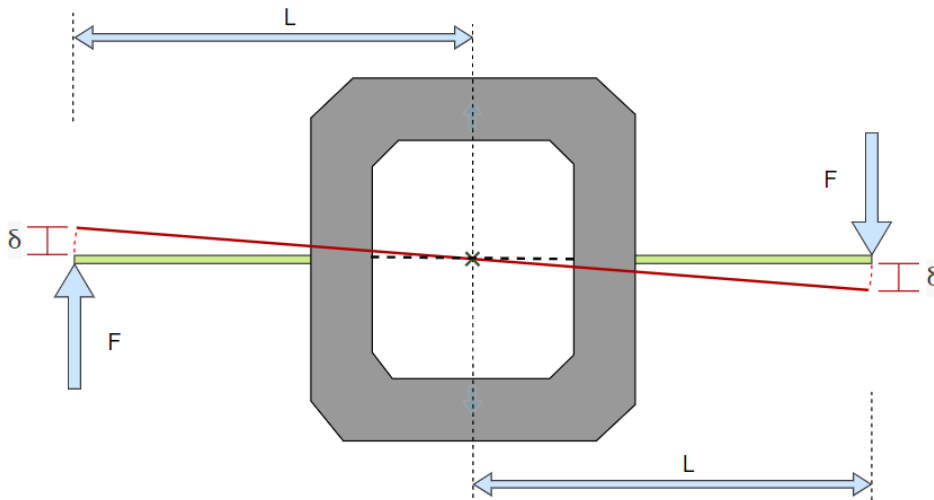
Figure 10: Diagram of torsional stiffness

2.5 DYNAMICS AND SUSPENSION LOADS

To perform a structural analysis of the monocoque, it was necessary to calculate the suspension loads that will be applied to the suspension points on the outer shell of the monocoque so that it can be correctly designed without major structural flaws.

2.5.1 *Vehicle Axis Systems*

Throughout the various dynamic situations, such as while accelerating, cornering, and braking, there is a weight transfer on the vehicle, this transfer occurs relative to a vehicle's center of gravity (CG) under accelerating or braking, and about the center of rotation when cornering. Presented in figure 11, one of the various Society of Automotive Engineers (SAE) coordinate systems, there are three axes on which there is displacement and rotation, the X axis is in the longitudinal direction to the front of the vehicle, the Y axis points to the driver's right side and the Z axis to the bottom of the vehicle.
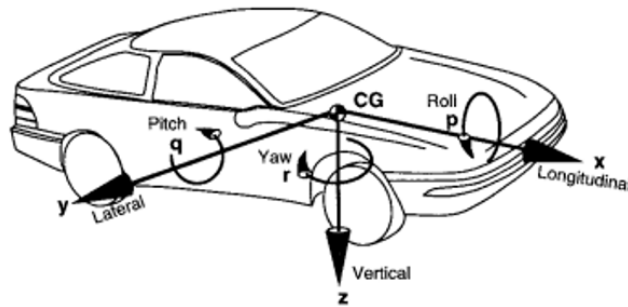
Figure 11: SAE vehicle axis system, adapted from[14]

When the vehicle is accelerating or braking there is a longitudinal weight transfer that is given through the equation 18, this weight transfer is also called the pitch that happens around the Y-axis.

$$\Delta W_{long} = \frac{W A_x h}{l},\tag{18}$$

Where ΔW_{long} corresponds to the weight gain on the rear axle, W is the weight of the vehicle, A_x is the longitudinal acceleration in g´s, taking into account that this value is positive for acceleration and negative when braking, h is the height of the CG to the ground and l is the wheelbase of the vehicle.

While cornering there is a lateral weight transfer over the rotation axis of the vehicle, this axis connects the front roll center to the rear roll center creating a imaginary rotation axis over which the vehicle will roll as it can be seen in the figure: 12, this movement is called roll, adopting a simplified method due to limited resources and information, it is possible to calculate this weight transfer through the equation 19 and 20:

W_s W REAR ROLL CENTER z_R (NRA)

FRONT ROLL CENTER

W_{uF} h_2

H θ

W_{uR} z_{RR}

z_R

+x h z_{WR}

z_{RF} z_{WF} h_s

ε

a_s

a b

ℓ

W_{uF} = Front unsprung weight (lb.), at height z_{WF} (ft.)
W_{uR} = Rear unsprung weight (lb.), at height z_{WR} (ft.)
W_s = Sprung weight (lb.), at height h_s and perpendicular
       distance h_2 from the NRA (ft.)
W = Total vehicle weight (lb.), at height h and vertical
       distance H from the NRA (ft.)
z_{RF}, z_{RR} = Front and rear roll center heights (ft.)
θ = Inclination of the Neutral Roll Axis (radians)

Figure 12: Lateral weight transfer on the roll axis, adapted from [14]

$$\frac{\Delta W_F}{A_y} = \frac{W}{t_F} \cdot \left[\frac{HK_F}{K_F + K_R} + \frac{b}{l} Z_{RF} \right], \tag{19}$$

$$\frac{\Delta W_R}{A_y} = \frac{W}{t_R} \cdot \left[\frac{HK_R}{K_F + K_R} + \frac{a}{l} Z_{RR} \right], \tag{20}$$

Where ΔW_F and ΔW_R corresponds to the weight gain between the wheels of the front and rear axle respectively.

Table 1: Detailed data of an FSAE vehicle, adapted from [15]

Variable	Value		Units
Total Mass of the Vehicle	W	330	(kg)
CG Height	h	0,37	(m)
Lateral acceleration	A_y	1,5	(g)
Longitudinal acceleration	A_x	1,2	(g)
Front Track Width	t_f	1,141	(m)
Rear Track Width	t_R	1,126	(m)
Wheelbase	l	1,55	(m)
Distance of CG to the Roll Axis	H	0,344	(m)
Front Roll Stiffness	k_F	114141,8	(N.m/rad)
Rear Roll Stiffness	k_R	88579,9	(N.m/rad)
Front axle distance to CG	a	0,593	(m)
Rear axle distance to CG	b	0,956	(m)
Height of Front Roll Center	Z_{RF}	0,02	(m)
Height of Rear Roll Center	Z_{RR}	0,037	(m)

Using the vehicle data shown in the table 1 presented above, its possible, trough the equations 18, 19 and 20 to calculate that the load transfer longitudinal is 94.53 kg, on the front is 70.43 kg and in the rear is 56.96 kg respectively.

2.5.2 *Suspension Systems and Features*

In this study, was used and adapted the suspension geometry present in the current FS vehicle (the T22).

The suspension has several purposes, such as:

- To provide vertical conformity between the wheels and the uneven road surface thus insulating the chassis from its irregularities;

- Maintain the suspension angles to provide greater grip between the tire and the road;

- Chassis rolling resistance;

- Keeping the tires in contact with the road in the various dynamic conditions of the vehicle, such as in a braking or cornering situation, maintains the greatest contact area of the tire with the road surface, thus providing the greatest amount of grip,

There are essentially two types of suspension: dependent and independent. In a dependent system, the two wheels are connected through a fixed axle, whereas in an independent system the two wheels can move freely away from each other allowing greater control of the vehicle as well as smaller dimensions and less mass.

The suspension geometry is what will determine how the vehicle will behave dynamically, although there are several types of suspension geometries available, generally, the most used in competition is the double wishbone suspension due to this being independent, the fact that it provides good support of longitudinal forces as well as transversal, low complexity of manufacture as well as excellent control of wheel movement, were some of the reasons why it is present in the formula student vehicle (figure 13) due to being a competition vehicle.

Figure 13: Suspension system of T22

The suspension has many variables that will affect its geometry which will change the vehicle´s dynamic behavior, as already mentioned above, the suspension system that will be used is a double wishbone suspension (figure 14), this type of suspension has 2 triangles, an upper and lower, also known as A-arms, responsible for connecting the upright to the chassis.
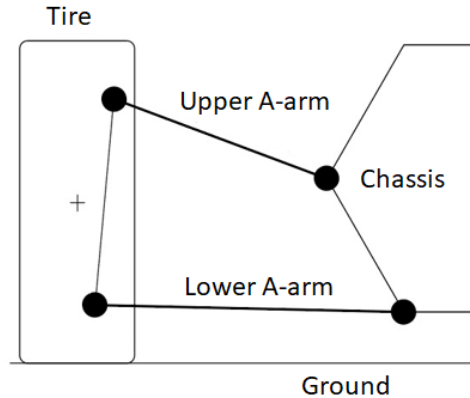
Figure 14: Exemplified schematic of a double wishbone suspension

There are two main suspension angles responsible for positioning the wheel on the road surface, these are camber and toe.

Camber refers to the inclination of the wheel relative to a vertical axis, perpendicular to the ground, this is one of the most important variables as it will influence the contact area of the tire with the ground, also known as the contact patch, thus increasing or decreasing the amount of grip available. As can be seen in the figure 15 the camber angle can be considered negative when the top of the wheel is tilted towards the center of the vehicle and positive when it is tilted outward.
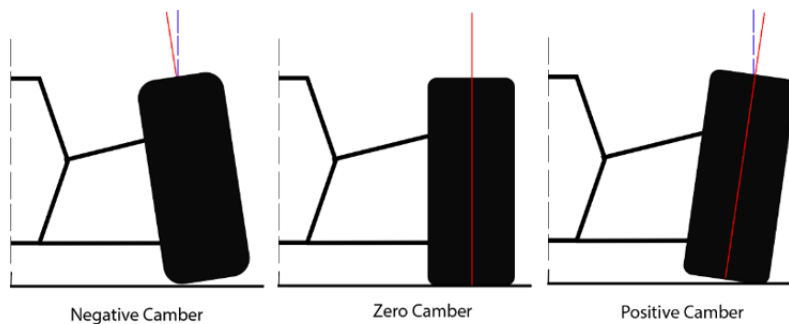
Figure 15: Camber angle

Toe, also known as tracking is defined by the inclination in the plane of the wheel center and the plane of the vehicle center in top view, in the figure 16 you can see when the wheels point to the center of the vehicle the wheels are at a negative angle (toe-in), if the wheels point out of the car it is at a positive angle (toe-out). Convergence will influence the stability of the vehicle in a straight line and in the curve, a car with toe-in on the front wheels will have more stability in a straight line, but less recession in changes of direction and vice-versa.
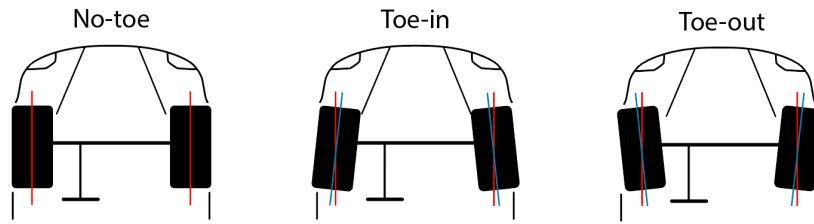
Figure 16: Toe or Tracking angle

In this type of suspension the other angles are directly incorporated in the upright, **the kingpin angle** (KPA), or kingpin inclination (KPI), is defined by the angle between the kingpin shaft and the vertical axis in front view, this is directly related to the drag radius, or **scrub radius**, as can be seen in figure 17, the hub length, or spindle length, corresponds to the distance between the wheel's center and the closest point on the upright.
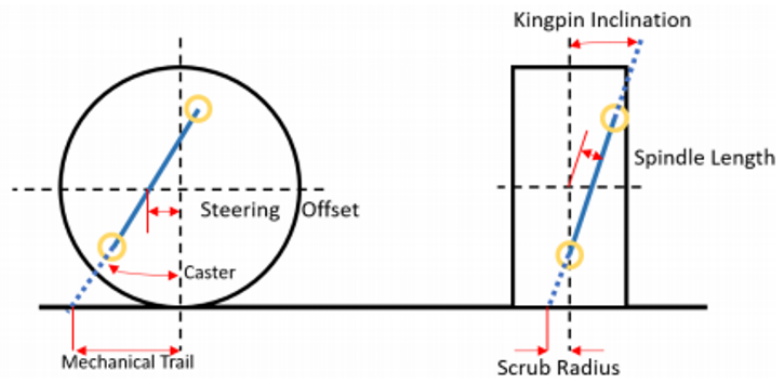
Figure 17: Kingpin and Mechanical trail, adapted from[16]

Caster is defined by the inclination of the upright axis relative to the vertical axis in the side view of the wheel as can be seen in the figure above, the caster is considered positive if the upright axis is inclined in the opposite direction of the vehicle, this if the vehicle is moving forward, this angle defines the **mechanical trail**, this is the distance from the vertical axis of the wheel to the projection of the upright axis on the ground.

2.5.3 *Tires*

The tire is one of the most important elements in the suspension system, based on **Thomas**[14] it is responsible for:

- Handle the vertical force while absorbing the irregularities of the ground;

- Develops longitudinal forces under acceleration and braking;

- Develops lateral forces in a curve,

A suspension must be designed around the tire, there is no point in a suspension working with a "perfect" geometry if it can't extract the maximum benefit from the tire and its ability to grip in various situations, this is why one of the first things to choose when designing a suspension is what tire is gonna be used.

In simpler analysis, tires are treated as a rigid body in order to simplify the transmission of the loads, but this method is not correct because the tire will deform in various dynamic situations, mostly while cornering, the contact patch deforms which will influence to the amount of grip it can offer. In a cornering situation it deforms in such a way that an angle appears between the central plane of the wheel and the direction in which the wheel is moving, this angle is known as the slip angle α, (figure 18) this is a very important characteristic of each tire that will influence the amount of grip that is available for each situation.
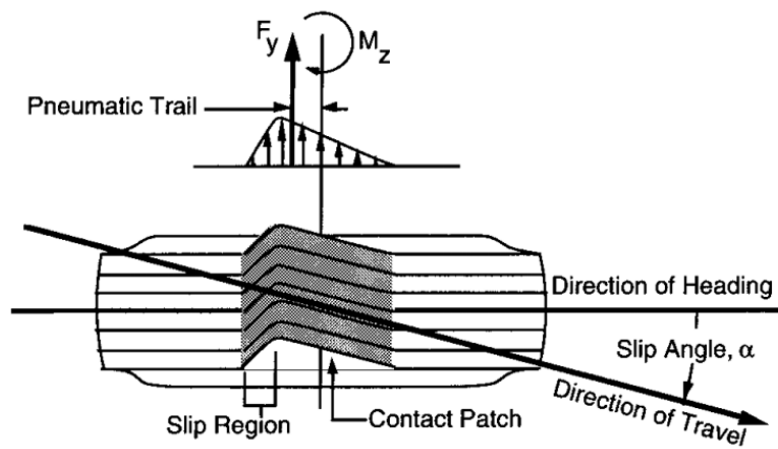
Figure 18: Tire contact patch with slip angle, adapted from [14]

It is important to mention that there is a relation between the tire's behavior in relation to the ground and the amount of lateral and vertical force that the tire can withstand, which is not a linear function, as can be seen in the graph present in the figure 19.

In order to maximize the performance of each tire, it is important that the tire works at an optimum slip angle so that it is able to deliver the maximum amount of lateral force, also commonly known as lateral grip.

One way to acquire the information for each type of tire is to buy the information from a testing laboratory that performs a series of tests on specialized analysis machines like the one shown in the figure 20, the one here exemplified is called the FSAE (Formula SAE) Tire Test Consortium (TTC). Due to this information being quite expensive, it will be used as information available for an equivalent tire in order to perform the correct calculations.

One example of a research center is the Calspan Tire Research Facility (TIRF), due to the high demand for the various fs teams, the center has conducted several tests for each type of tire most commonly used in motorsport.
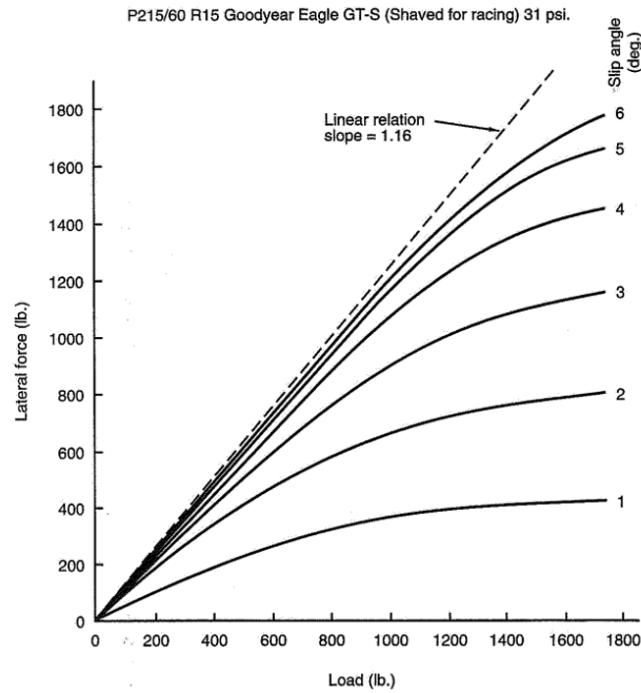
Figure 19: Example graph of vertical load versus lateral force with a range of slip angles, adapted from [14]

Figure 20: Calspan TIRF tire measurement machine, adapted from [17]

For each tire, several tests are performed where the objective is to show the information of the tire when it is rolling freely, while in a cornering situation, accelerating, and braking. In figure 21, it is possible to observe the terminology used by SAE regarding the planes and axis used in order to facilitate the interpretation of the forces and moments experienced by the tire, these correspond, together with other data such as the different temperatures, humidity, etc..., to the data obtained through experimental testing.

In the test, some of the variables are already predefined like the vertical load F_z that will be applied on the tire as well as the tire camber, through these it is possible to discover the lateral force F_y with the variation of the slip angle and the longitudinal force F_x available.
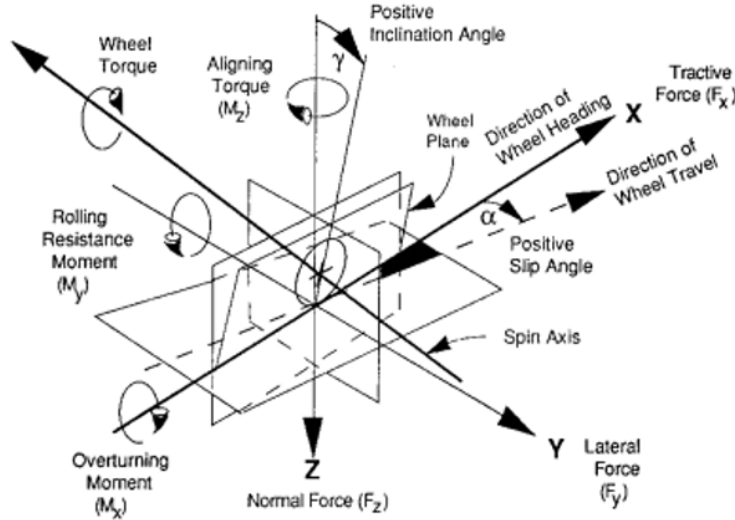
Figure 21: Diagram of forces and moments on a tire in the SAE standard system, adapted from[14]

The rollover moment M_x comes from the lateral force creating a moment about the wheel center. Despite all the variables that are provided through FSAE TTC, the ones needed for a finite element analysis of the suspension are F_x, F_y, and M_z also known as the alignment torque.

2.5.4 *Suspension Loads Calculations*

By adapting the research conducted by **Lane Thomas** [18] and applying it to the work in question was possible, through the use of vector calculation and static equations, to calculate the various forces applied at various points of attachment of the suspension. The nomenclature used for the calculation is shown in the figure 22, as well as the representative diagram of the suspension in question, as mentioned above the suspension in question is a double wishbone with 4 links plus the arm that connects to the shock absorber plus another one that controls the toe, all the arms present in the suspension system will only work in tension and compression eliminating any kind of axial or bending forces from the calculation. The Lower A-Arm is composed of the vectors *EA* and *EB*, the upper A-Arm corresponds to the vectors *FC* and *FD*, and the push-rod and the toe arm corresponds to the vectors *GH* and *JK* respectively.

As already discussed above for the calculations of the suspension forces/loads, the information taken from the FSAE TTC that was available was from the tire Goodyear D2692 20x7.0-13. The forces used in this study are forces that have as their origin the surface of the tire that is in contact with the ground, which in turn will be transmitted to the center of the wheel. The next step was to divide this force by the various suspension members using vector calculation.

In the table, 2 are the coordinates of the suspension points that were used for this study of forces for both the front and rear suspension.
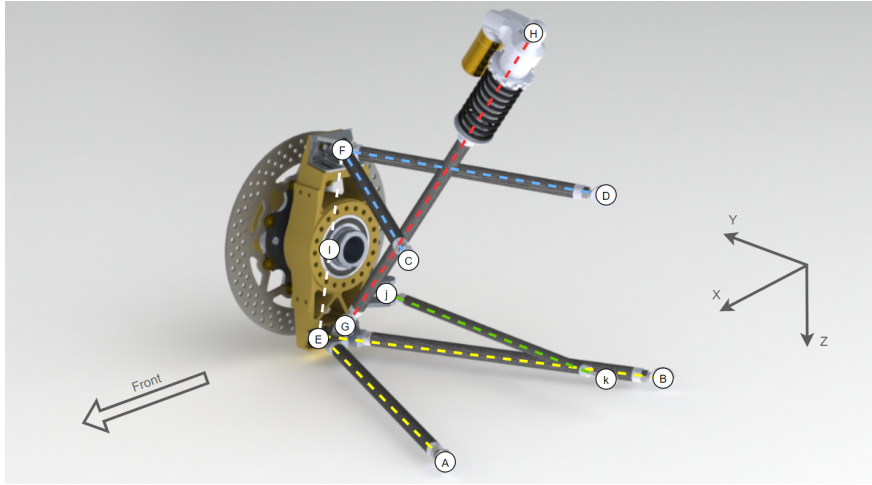
Figure 22: Diagram of the suspension vectors used for the loads calculation

Table 2: Suspension points coordinates

Suspension	Frontal			Rear		
Points	X	Y	Z	X	Y	Z
A	- 0,404	0,215	- 0,066	- 1,913	0,280	- 0,052
B	- 0,733	0,215	- 0,066	- 2,195	0,280	- 0,052
C	- 0,424	0,285	- 0,264	- 1,913	0,280	- 0,223
D	- 0,716	0,285	- 0,264	- 2,195	0,280	- 0,223
E	- 0,557	0,588	- 0,077	- 2,107	0,579	- 0,076
F	- 0,573	0,554	- 0,297	- 2,173	0,548	- 0,296
G	- 0,562	0,542	- 0,097	- 2,119	0,503	- 0,307
H	- 0,558	0,229	- 0,485	- 2,119	0,231	- 0,441
I	- 0,565	0,571	- 0,187	- 2,120	0,563	- 0,186
J	- 0,624	0,554	- 0,117	- 2,048	0,567	- 0,112
K	- 0,625	0,180	- 0,117	- 2,150	0,280	- 0,080

The first step in calculating the forces was, using as an example of the arm EA, to take the coordinates from each point (equation 21) and create the vector EA (equation 22) that represents the connection from point E to A as well as its magnitude vector ea (equation 23) that will allow for calculating the unit vector η_{EA} (equation 24).

$$E = \lfloor E_x, E_y, E_z \rfloor \tag{21}$$

$$EA = \left[E_x - A_x, E_y - A_y, E_z - A_z \right] \tag{22}$$

$$ea = \sqrt{(E_x - A_x)^2 + (E_y - A_y)^2 + (E_z - A_z)^2} \tag{23}$$

$$\eta_{EA} = \left[\frac{EA_x}{ea}, \frac{EA_y}{ea}, \frac{EA_z}{ea} \right] \tag{24}$$

The same procedure was used in order to calculate a unit vector for each arm shown in the figure 22, that in the end will result in six unit vector η_{EA}, η_{EB}, η_{FC}, η_{FD}, η_{GH} and η_{JK}. By admitting this is a static analysis, the sum must equal 0. In the equation, 25 can be seen the summation of the forces in the X direction.

$$\sum F_x = 0 = F_{EA}\eta_{EA_x} + F_{EB}\eta_{EB_x} + F_{FC}\eta_{FC_x} + F_{FD}\eta_{FD_x} + F_{GH}\eta_{GH_x} + F_{JK}\eta_{JK_x} + F_X \tag{25}$$

The F_x will represent the forces in the X direction that is being applied, by the tire, in the center of the upright, the same for the forces in the Y direction (F_y) and Z direction (F_z).

Despite knowing three equations ($\sum F_x$, $\sum F_y$ and $\sum F_z$), there are still six unknown ones, in order to calculate the moments around the wheel center, was necessary to create an additional three static equations, using the center of the wheel as the starting point (point I), vectors connecting the center of the wheel to the four outboard suspension points of the two A-arms, i.e., points A, F, G and J will be created and named r (equation 26).

$$r_E = E - I = \left\lfloor r_{E_x}, r_{E_y}, r_{E_z} \right\rfloor . \tag{26}$$

To sum the moments about the wheel center, the r vectors for each point were crossed with the F vectors from the equation 25, which for the X direction is obtained in the equation 27, where M_x corresponds to the moment at the wheel center from the different loading scenarios.

$$\sum M_x = 0 = F_{EA}\left(\eta_{E_z}r_{E_y} - \eta_{E_y}r_{E_z}\right) + F_{EB}\left(\eta_{E_z}r_{E_y} - \eta_{EB_y}r_{E_z}\right) + F_{FC}\left(\eta_{FC_z}r_{F_y} - \eta_{FC_y}r_{F_z}\right)$$
$$+ F_{FD}\left(\eta_{FD_z}r_{F_y} - \eta_{FD_y}r_{F_z}\right) + F_{JK}\left(\eta_{JK_i}r_{K_y} - \eta_{JK_y}r_{K_z}\right) + F_{GH}\left(\eta_{GH_z}r_{G_y} - \eta_{GH_y}r_{G_z}\right) + M_X \tag{27}$$

By repeating the equation above for the Y direction (M_y) and Z direction (M_z), the forces in the six suspension members were calculated. The format of the equation is given by the equation 28 where the three necessary members for this calculus can be seen in the equations 29, 30, 31 and 32.

$$[[A]|[B]]\{x\} = \{b\} \tag{28}$$

$$[A] = \begin{bmatrix} \eta_{EA_X} & \eta_{EB_X} & \eta_{FC_X} \\ \eta_{EA_Y} & \eta_{EB_Y} & \eta_{FC_Y} \\ \eta_{EA_Z} & \eta_{EB_Z} & \eta_{FC_Z} \\ \eta_{EA_Z}r_{IE_Y} - \eta_{EA_Y}r_{IE_Z} & \eta_{EB_Z}r_{IE_Y} - \eta_{EB_Y}r_{IE_Z} & \eta_{FC_Z}r_{IF_Y} - \eta_{FC_Y}r_{IF_Z} \\ \eta_{EA_Z}r_{IE_X} - \eta_{EA_X}r_{IE_Z} & \eta_{EB_Z}r_{IE_X} - \eta_{EB_X}r_{IE_Z} & \eta_{FC_Z}r_{IF_X} - \eta_{FC_X}r_{IF_Z} \\ \eta_{EA_Y}r_{IE_X} - \eta_{EA_X}r_{IE_Y} & \eta_{EB_Y}r_{IE_X} - \eta_{EB_X}r_{IE_Y} & \eta_{FC_Y}r_{IF_X} - \eta_{FC_X}r_{IF_Y} \end{bmatrix} \tag{29}$$

$$[B] = \begin{bmatrix} \eta_{FD_X} & \eta_{JK_X} & \eta_{GH_X} \\ \eta_{FD_Y} & \eta_{JK_Y} & \eta_{GH_Y} \\ \eta_{FD_Z} & \eta_{JK_Z} & \eta_{GH_Z} \\ \eta_{FD_Z}r_{IF_Y} - \eta_{FD_Y}r_{IF_Z} & \eta_{JK_Z}r_{IK_Y} - \eta_{JK_Y}r_{IK_Z} & \eta_{GH_Z}r_{IJ_Y} - \eta_{GH_Y}r_{IJ_Z} \\ \eta_{FD_Z}r_{IF_X} - \eta_{FD_X}r_{IF_Z} & \eta_{JK_Z}r_{IK_X} - \eta_{JK_X}r_{IK_Z} & \eta_{GH_Z}r_{IJ_X} - \eta_{GH_X}r_{IJ_Z} \\ \eta_{FD_Y}r_{IF_X} - \eta_{FD_X}r_{IF_Y} & \eta_{JK_Y}r_{IK_X} - \eta_{JK_X}r_{IK_Y} & \eta_{GH_Y}r_{IJ_X} - \eta_{GH_X}r_{IJ_Y} \end{bmatrix} \qquad (30)$$

$$\{x\} = \begin{Bmatrix} F_{EA} \\ F_{EB} \\ F_{FC} \\ F_{GH} \\ F_{JK} \\ F_{GH} \end{Bmatrix}, \qquad (31)$$

$$\{b\} = \begin{Bmatrix} F_X \\ F_Y \\ F_Z \\ M_X \\ M_Y \\ M_Z \end{Bmatrix}, \qquad (32)$$

By adapting the tire data provided by **Thomas** to the problem in question, the forces in the arms were calculated.

It should be noted that the method used to calculate the suspension forces is a simplified method that does not take into account several variables present in this system such as the degrees of freedom of the joints that are located at the end of each suspension arm, as well as not considering the steering angle that will influence all the forces transmitted in a cornering situation.

Taking these aspects into account, a safety factor was applied in order to create a margin so that on track there is no danger of the forces being greater than what the shell can handle and risking the safety of the driver.

MONOCOQUE DESIGN

3.1 INITIAL CONSIDERATIONS

To start drawing and sketching the geometry of the monocoque itself, was needed to have many things in consideration such as the main components that will be assembled into it, like the battery, the engines, the suspension geometry, etc... all those that will be applying big loads on the inside such as on the outside shell.

As previously mentioned above, one of the biggest reasons to develop and build a carbon fiber monocoque it´s its big advantage in using a good ratio of weight to stiffness materials, this translates into a very lightweight yet very strong and stiff structure that improves the dynamic of the vehicle reducing the amount of sprung mass. The development of a good monocoque structure goes through a lot of iterations in order to achieve the design that best fits the team's necessities.

3.1.1 *FSAE Rules*

Being a motorsport competition between various university teams, both have to respect and be in compliance with the rules [19] that are stipulated by the FSAE in order to take place in this competition. There are specific guidelines regarding obligatory dimensions of the chassis like the ones shown in figure 23. The rules also provide a template regarding the dimension and the ergonomics of the driver, figure 24 shows the 95th percentile of the male sex, all of these dimensions are very important, first of all, to assure the safety of the driver, and also for the teams to have an idea of how the driver is positioned inside of the vehicle. Both of these templates have to be inserted inside the chassis during scrutineering to ensure compliance with the rules.
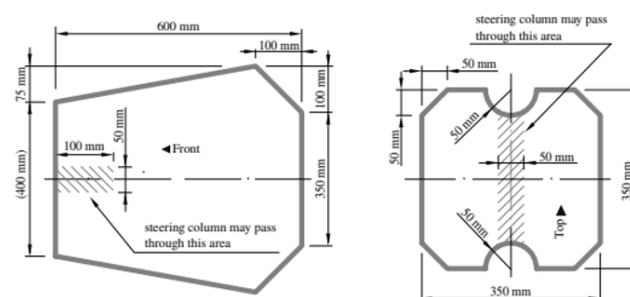
Figure 23: Template FSAE cockpit openings, adapted from[19]
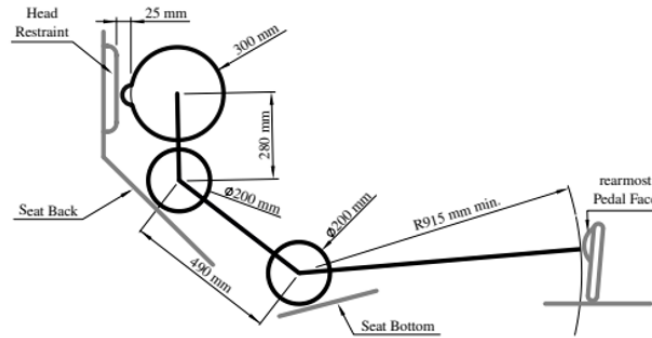
Figure 24: Template FSAE 95th percentile, adapted from[19]

3.1.2 *Suspension Attachment Points*

There are several different variations of the type of support from each team as shown in the figure 25, however, despite being a small part, these are very important as this is one of the principle link elements of the suspension between the upright and the monocoque outside shell which is responsible for handling forces around 7000 Newtons during cornering, accelerating and braking.

Figure 25: Example of suspension attachment points, adapted from[20]

For this project, it was also designed and developed this part (figure 26) in order to study the suspension forces on a carbon fiber sandwich laminate, the geometry of this part is also very important because it helps for the forces dissipate through the shell and not focusing in just one specific point.
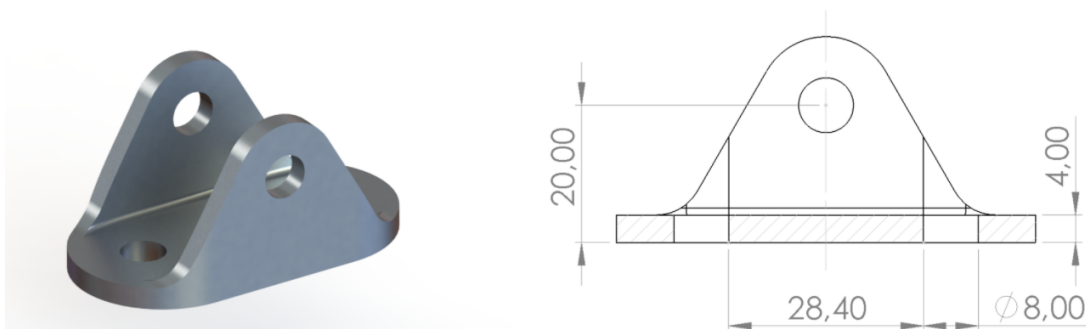
Figure 26: Designed suspension attachment part

3.1.3 *Powertrain and Battery*

Since the monocoque will be developed to be an electric vehicle, it needs to be able to accommodate the accumulator, this includes the battery module which includes the lithium cells, the battery management system (BMS), etc... the two electric motors, since the team is planning to use two motors in the rear, one for each wheel, in order to avoid using a differential a tighter package overall and the inverters to control the motors.

By conducting research on the market, the powertrain department has made the decision of using a pair of EMRAX 188 shown in figure 27, these motors comply with the requirements stipulated by the teams in many terms such as performance, being very compact due to them being axial motors and these are also very efficient compared to other electric motors in the market.

Figure 27: Electric motor - EMRAX 188, adapted from[21]

Regarding the choice of the inverters, these were chosen in addition to their nominal values, i.e. in terms of rated voltage compatibility, maximum currents, switching frequency, etc... but also due to the fact that they already have bench validation by several companies and FS teams. According to these requirements, it was concluded that the BAMOCAR D3 (figure 28) would be the best choice for the team.

Figure 28: Inverter - BAMOCAR D3, adapted from[22]

For the battery, several calculations were performed to find the energy capacity required for the battery, this specific value was obtained through various lap time simulations to discover what was the energetic efficiency in order to reach the required discharge current and voltage in order to obtain the power and respect the rated values of the motor.

Based on the calculations of the parameters mentioned above, it was possible to determine, throughout several iterations of different arrangements of the cells (SAMSUNG 25R) in parallel and series in order to obtain the minimum dimensions for the battery pack also known as the accumulator, this pack already accounts the entire cooling system and peripherals such as the BMS, contactors, fuses, busbars, etc... as exemplified in the figure 29.
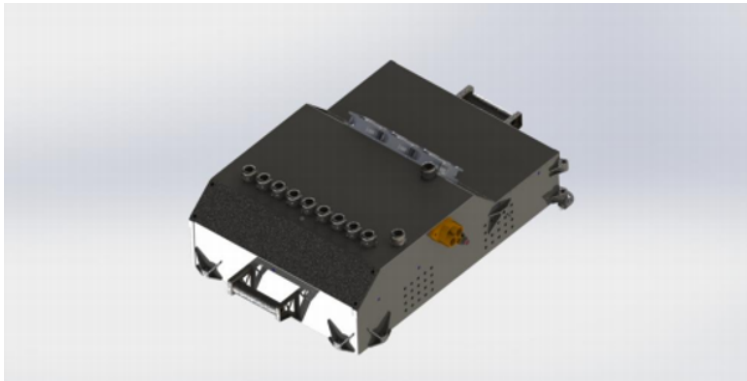
Figure 29: Battery pack - cccumulator, adapted from [23]

3.2 MATERIALS SELECTION

3.2.1 *Fiber Materials*

As was already previously mentioned above, the reinforcement used was carbon fiber. Due to the big developments in the area of composites, there is a great variety of different fibers depending on the application as well as its composition. This choice is usually very limited to the team's available budget for this area such as if the supplier would help with the costs overall or not.

There are a variety of methods that could be used for the manufacturing of the monocoque, there are three types that are the most common amongst others like prepreg, wet-layup, and infusion as shown in the figure 30 respectively. Regarding the use of pre-impregnated fibers, despite being more expensive, it is easier to handle in the lamination process, making the process cleaner, as the resin is already in the fiber, as well as reducing the probability of errors such as bridging, miss alignment, and voids, which may weaken the structure in small localized points that in the future could result in failure.

Knowing what process will be used for the manufacture of the structure of the monocoque, a search was made around what other teams normally use as well as why they use it and what are the requirements for makings this choice.
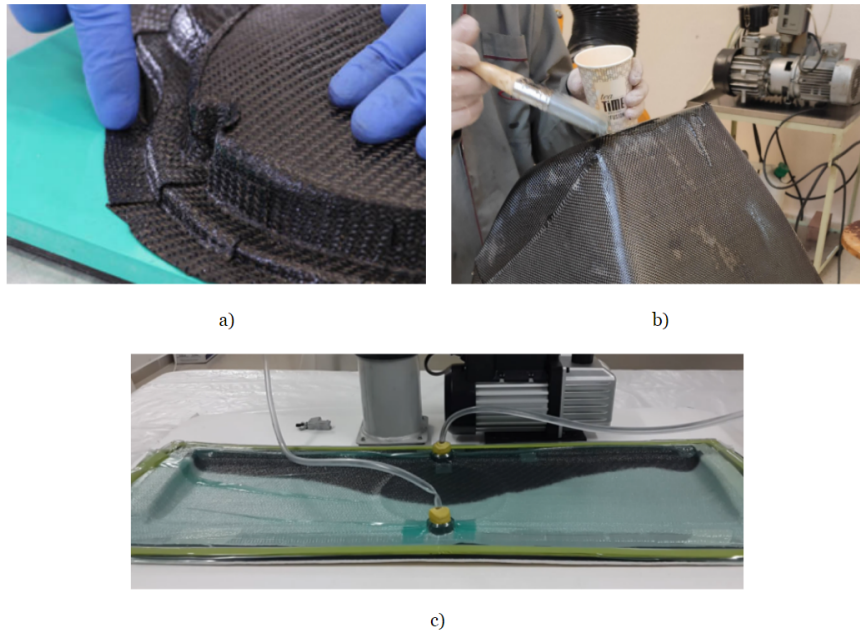
Figure 30: Types of carbon fiber layups: a) Prepreg, adapted from [24], b) Wet-layup, and c) Infusion, adapted from [25]

After making this search, it was noticed that the trend was to use medium-weight fibers with more layers so that the load is distributed over more layers which results in overall better strength, and also due to some of the complex shapes present in this type of structures. Taking this into account, it was decided to use the XC130 210g for this project, as was already mentioned, this is a pre-impregnated fiber with 210 of grammage which requires an autoclave or a woven with vacuum exits to cure, this is a woven cloth with a pattern of 2x2 as it is shown in the figure 31, this fiber is commonly used in various applications where a good finish is needed as well as good structural integrity.
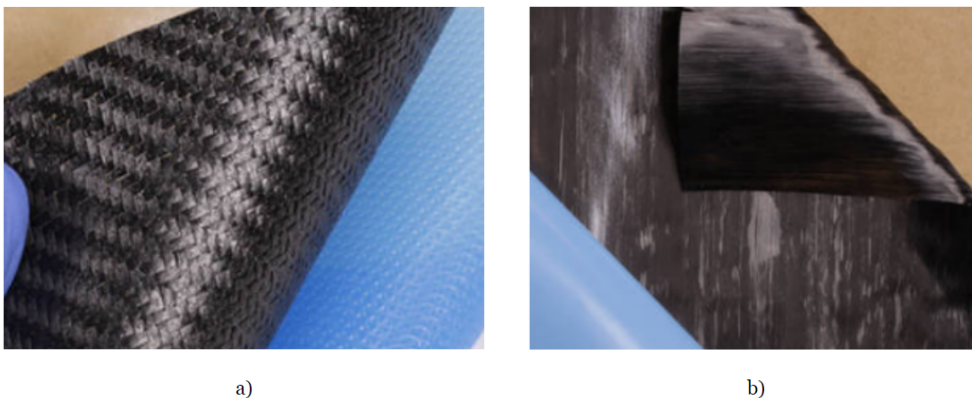
Figure 31: Types of fibers: a) Woven, b) Unidirectional, adapted from [24] and [26] respectively

To reinforce the areas that will be subjected to higher bending forces, it was decided to use unidirectional fibers, also pre-impregnated, unlike woven fabrics, this type of fiber has all the fibers aligned in just one direction as can be seen above (figure 31), this provides very high strength in on the desired direction. For this study it will be used the MTC510 - UD300, this is a fiber with high tensile and compressive strength.

3.2.2 *Core Materials*

Due to being a sandwich-like type structure, it is necessary to choose what will be used, as was already mentioned above, the main objective of using a sandwich-like type of structure is to increase the cross-section of the structure and increase the distance from the plies to the center line which will results in a higher flexural modulus overall. There are numerous choices for this use, like using a honeycomb structure (figure 32) made out of a very thin aluminum sheet as well as using different densities of foams (figure 32) like polyurethane (PU), polystyrene (PS) to polyethylene terephthalate (PET) which is one of the most recent foams that has an outstanding price to performance ratio.

a)   b)
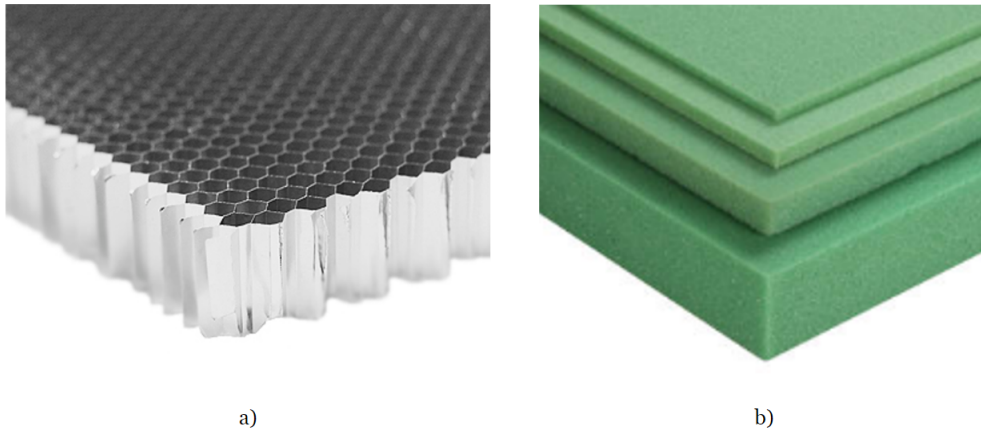
Figure 32: Types of cores: a) Honeycomb structure, b) Structural foam, adapted from [27] and [28] respectively

For this specific study, it was decided to use the honeycomb aluminum structure for several reasons such as the stiffness to weight is really good in this type of material, the fact that it is easier to mold it into the needed curves, despite this type of core having a lower contact area with the laminate than the foam, the use of a pre-impregnated fiber, that uses an autoclave to cure, allows the use of a structural adhesive mentioned below, etc...

There are several types of densities of the cells available for the honeycomb, most common are 1/8" and 1/4" for this type of application, this density will contribute to a higher compressive strength of the panel, whereas the thickness of the core will influence the flexural stiffness of the overall panel. In this case, was used the properties for a 1/8" cell size means that the distance of two of six opposite walls in a hexagonal arrangement is 1/8" (or 3.175 millimeters).

3.2.3 *Insert Materials*

In order to be able to mount various attachments to the monocoque, like the main hoop, suspension points, belts, pedal box, etc... it is required the use of inserts to prevent the crushing of the core in the sandwich structure, is also worth mentioning that is not allowed any damage to the core in panels, as mentioned in the point T.3.16.5 in the FSAE rules[19].

Any attachment points that use bolt-on joints must use a material with a very high compression strength, these inserts can be made out of many materials, various sizes and dimensions as long as they comply with the rule mentioned above.

In the case at hand, were used aluminum inserts (figure 33 a)), since this type of material has a high compression resistance and in order to simplify the development and structural study of the mono, these were used, as already mentioned, not only in the suspension points but also in critical points subject to large forces such as the pedal attachment points, harnesses, roll-over hoops, etc... In order to optimize even further the weight saving the inserts can be extremely optimized whether in its geometry (figure 33 b)) or on the materials of itself.

a)   b)
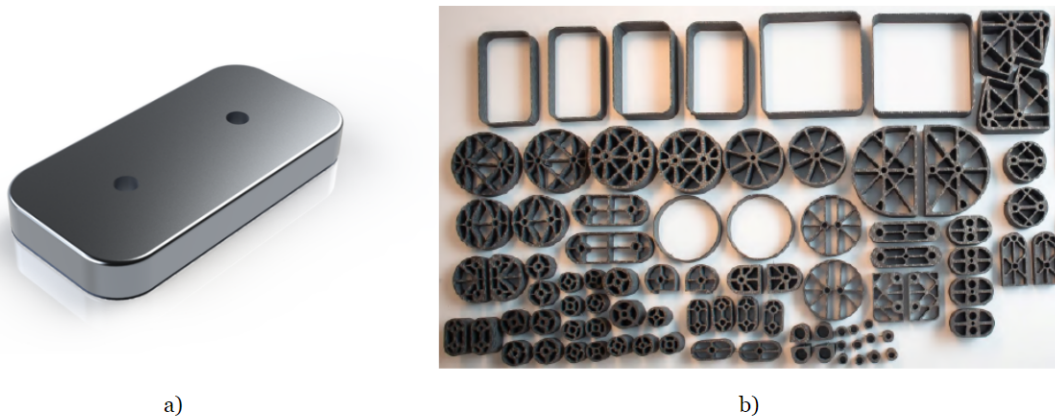
Figure 33: Inserts examples: a) Aluminium insert, b) NTNU waterjet cut optimized inserts, adapted from [29]

For the other attachment points, where the load to which they will be subjected is not as critical and high, there are several studies conducted to reduce the weight of the inserts without having to compromise on overall strength. Within these options, we have inserts composed of forged carbon fiber as researched by João [29], as can be seen in the figure 34, in addition to this method is also possible through the use of three-dimensional (3D) printing to create very resistant inserts without using generic materials, due to the wide variety of materials that can be printed today through processes such as Fused Deposition Modeling (FDM), Stereolithography (SLA), etc ...

Figure 34: Example of forged carbon fiber inserts, adapted from [29]

3.2.4 *Adhesive Materials*

Due to the nature of the process, it is necessary that, between the layers of pre-impregnated carbon fiber, and honeycomb core, the use of an adhesive to bond the 2 components together, this adhesive will be applied during the process of lamination together with the honeycomb structure, this type of adhesive also requires an autoclave to cure, after the curing process the adhesive will secure the core like shown in the figure 35.
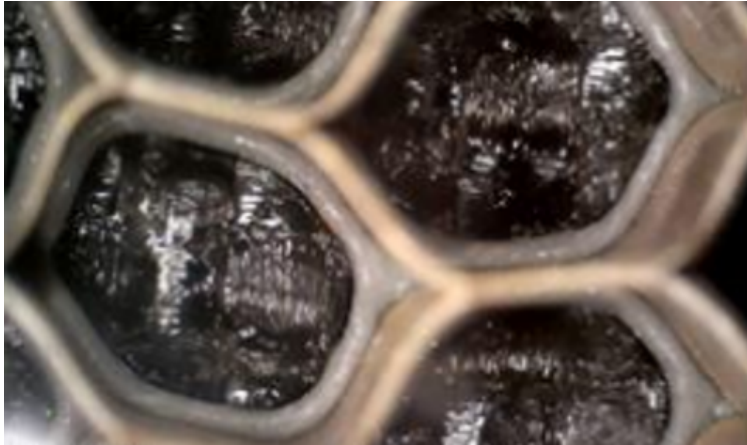
Figure 35: Adhesive on a honeycomb structure after the curing process, adapted from[30]

3.3 STRUCTURAL LAMINATE ANALYSIS

Safety is one of the major concerns in motorsport, for that, and many more reasons there are several standards not only for the mandatory chassis dimensions, as mentioned above but also for the composition of the panels that make up the main structure of the chassis if using an alternative material to steel tubes.

One of the many reasons for developing and manufacturing a monocoque is to replace a conventional steel space frame chassis, for this to happen the carbon fiber structure must comply with the regulations (table 3), regarding its ability to withstand the loads that will be applied to it.

In the initial part of the rules, it is defined which steel tubes can be used in the various areas of the structure and, based on this data, the panels of the monocoque will have to have equivalent strength and stiffness depending on the area, where they will be applied, in figures 36, is possible to see two of the tests imposed by the regulation, the first one being a three-point bending test (3PBT) that tests the bending capabilities of the panel and the second a perimeter shear test (PST) that is responsible to test the perimeter shear strength (PSS) of the panel.

Table 3: FSAE test requirements, adapted from [19]

Tests	FSAE Rules Requirements
Three Point Bending Test (3PBT)	Test panel dimensions: 275 x 500 mm; Load applicator must have a 50 mm radius; Distance between supports of 400 mm;
Perimeter Shear Test (PST)	Test panel dimensions: 100 x 100 mm; Load applicator must have 25 mm of diameter; Fixed support with 32 mm hole
Side Impact Structure (SIS)	EI and absorbed energy of the vertical panel equivalent to 2 steel tubes; PSS = 7.5 KN; EI and absorbed energy of ½ of floor panel equivalent to 1 steel tube;
Front Bulkhead (FB)	PSS equivalent of a 1.5 mm steel plate; EI equivalent to 2 steel tubes;
Front Bulkhead Bracing Supports (FBHS)	EI vertical single panel equivalent to 1 steel tube; Total EI of FBHS equivalent to 6 steel tubes; PSS = 4.0 KN;
Any Primary Structure Attachment Points to the Monocoque	Withstand 30 KN in any direction;
Harness Attachment Points	Shoulder and Legs Harness: 13 KN in any direction; Anti-submarine Harness: 6.5 KN in any direction;

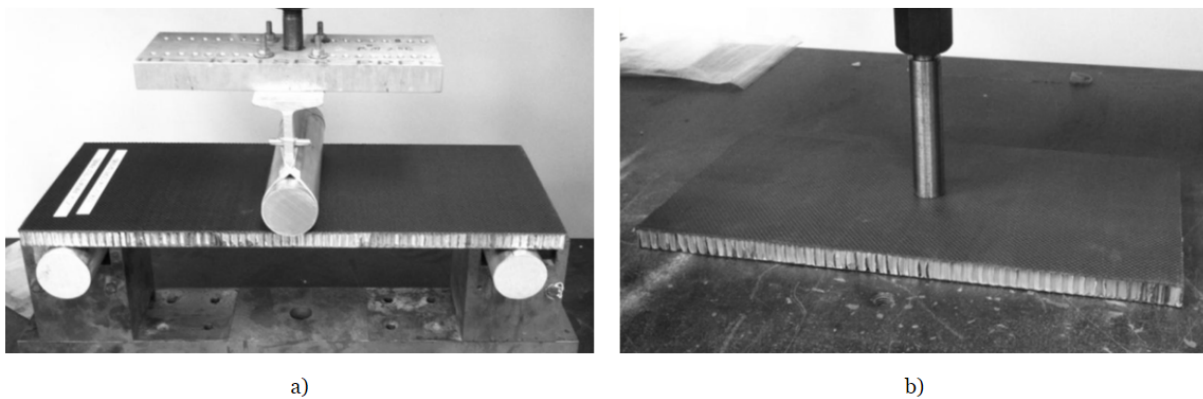a)   b)

Figure 36: Example of the required tests a) 3PBT, b) PST, adapted from [31]

The main objective for performing this test, is to determine, as previously mentioned, the bending properties of the sandwich panel, also known as flexural stiffness (EI), the higher the value, the better the performance under a bending force.

For this test to be valid, according to the FSAE protocols, the rig has to have specific dimensions for the panel, load applicator and the distance between supports, as described in the table 3, and in the figure 37.

The load applicator will apply a force in the middle of the panel, that will lead to a specific displacement (δ), which will allow to determine the *EI* for the panel being tested, the bending stiffness is directly related to the laminated panels present in the sandwich structure. The resulting graph from this test is almost a straight line, with normally a flat spot in the end, that translates into the maximum load that results into failure, this happens due to the high stiffness of this type of materials.
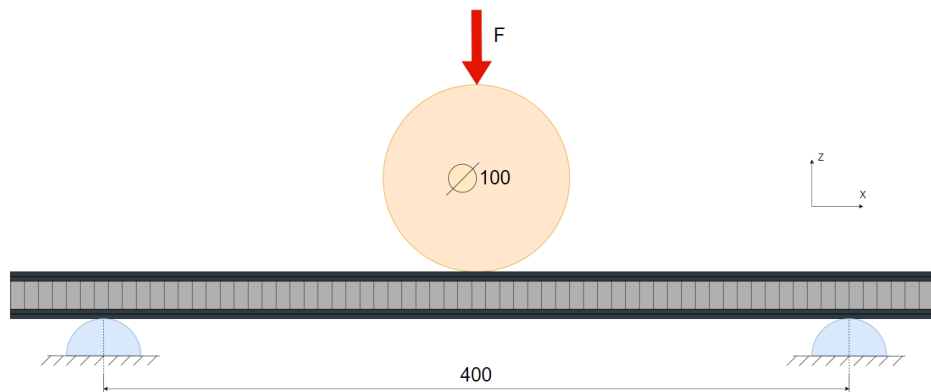
Figure 37: Diagram of a three point bending test

For a PST, the objective is to determine the shear strength of the sandwich panel, in the table 3 and figure 38, can be seen some requirements imposed by the FSAE rules, the load applicator will apply a force in the center of the specimen, and will not stop until it goes through all the panel to determine the failure load for the upper and lower laminate, the resulting graph from this test is a curve with two peaks that translate to the failure of both laminates, respectively, in a sandwich panels.
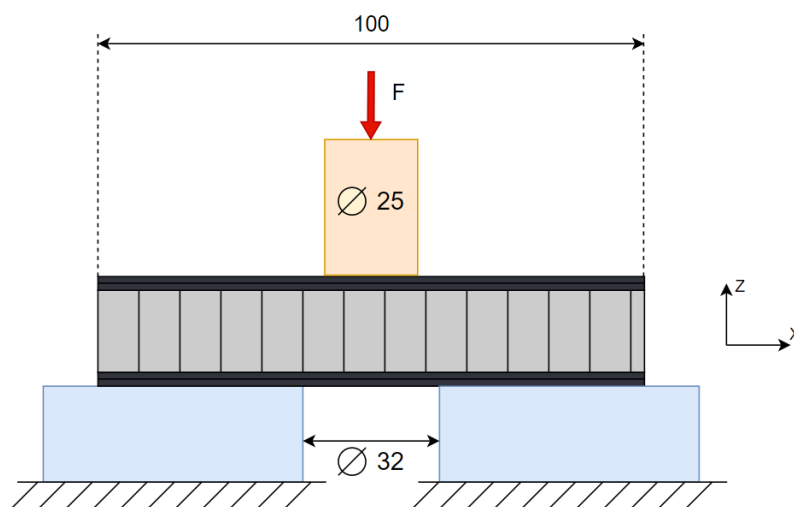
Figure 38: Diagram of a perimeter shear test

In order to know if the structure would comply with the regulations[19], was necessary to calculate the flexural stiffness of a steel tube using the equations 33, as well as other variables like the force-deflection relation, known (G_s), and the absorbed energy capabilities (U_s), both for the steel, tube presented in the equation 34 and 35 respectively.

All the equations are provided from a structural equivalency spreadsheet (SES) [15], directly provided for the teams by the FSAE, so that they use all the same criteria for the selection of the structural panels.

$$EI = E . \tfrac{\pi}{64} . (D^4 - d^4), \tag{33}$$

$$G_s = \tfrac{F_{s2} - F_{s1}}{y_{s2} - y_{s1}}, \tag{34}$$

$$U_s = \sum_{i=0}^{n} (y_i - y_{i-1}) . F_i, \tag{35}$$

Where:

- EI = Flexural Stiffness;

- E = Young´s Modulus by the rules is 200 GPa;

- D = Steel Tube Outer Diameter;

- d = Steel Tube Inner Diameter;

- G_s = Force-Deflection Relation;

- F_{s1} = Force at no Deflection;

- F_{s2} = Force at 12.7 mm deflection;

- y_{s1} = 0 mm;

- y_{s2} = 12.7 mm, dictated by the FSAE Rules;

- U_s = Absorbed Energy in the steel tube;

- y_i = Displacement at a given Point;

- F_i = Force at a given Point.

For the laminate analysis since it is an assembly of different materials into a sandwich structure, in this case, carbon fiber for both upper and lower laminate, and honeycomb for the core, it requires other equations to determine the EI of the panel.

In classical mechanics, the force-displacement relation of a simply supported beam with symmetrical load, this is, the load is applied through the middle line on a beam, is given by the equation 36.

$$\delta = \frac{F.L^3}{48.E.I},$$
(36)

Where:

- δ = Displacement of the structure;

- F = Applied Force;

- L = Distance Between Supports;

- I = Moment of Inertia,

The Young´s Modulus, and Moment of Inertia, for a composite laminate structure, are calculated through the equation 37 and 38.

$$E = \frac{G_c.L_c^3}{48.I_c},$$
(37)

$$I_c = \frac{b.(h+t_1+t_2)^3 - h^3*b}{12},$$
(38)

$$G_c = \frac{F_{c2}-F_{c1}}{y_{c2}-y_{c1}} + S_c,$$
(39)

Where:

- L_c = Distance Between Supports;

- I_c = Moment of Inertia of the Composite;

- b = Width of the Panel;

- h = Thickness of the Core;

- t_1 = Thickness of the Upper Laminate;

- t_2 = Thickness of the Lower Laminate;

- G_c = Force-Deflection Relation;

- F_{c1} = Force at Point 1;

- F_{c2} = Force at Point 2;

- y_{c1} = Displacement at Point 1;

- y_{c2} = Displacement at Point 2;

- S_c = Setup Compliance of the test rig, it is a non-dimensional parameter to compensate for any unreliability of the test setup;

3.3.1 *Analysis Methodology*

Firstly, through the use of classical composite laminate theory [32] and matrix calculus, such as the use of the matrix $[ABD]$, was determined a laminate that would have a flexural stiffness (EI) that would be in compliance with the rules, through the determination of the displacement imposed by a force that would be applied into it.

The laminate compliance matrix (equation 40), also commonly referred to in classical laminate theory as the matrix $[ABD]$, consisting in the $[A]$, $[B]$, and $[D]$ matrices. The laminate compliance matrix is used to express laminate mid-plane strains (ϵ) and laminate mid-plane curvatures (k) in terms of laminate resultant forces per unit width (N) and laminate resultant moments per unit width (M).

$$
\begin{Bmatrix} N_x \\ N_y \\ T_{xy} \\ M_x \\ M_y \\ M_{xy} \end{Bmatrix} = \begin{bmatrix} [A] & [B] \\ [B] & [D] \end{bmatrix} \cdot \begin{Bmatrix} \varepsilon_{0x} \\ \varepsilon_{0y} \\ \gamma_{0xy} \\ \frac{\partial^2 w_0}{\partial x^2} \\ \frac{\partial^2 w_0}{\partial y^2} \\ \frac{\partial^2 w_0}{\partial x \partial y} \end{Bmatrix}
\tag{40}
$$

The laminate used in the analysis were most cases symmetrical, this means that the matrix $[B]$ is null due to the fact that it represents the correlation of properties with effects on displacements, given the existence of a plane tensile or bending stress.

Each analysis started with a basic laminate such as ($Bi_0/Bi_{45}/Bi_{-45}/Bi_0/Core/Bi_0/Bi_{-45}/Bi_{45}/Bi_0$), where Bi_0, Bi_{45}, and Bi_{-45} represent a woven bidirectional carbon fiber cloth at 0, 45, and -45 degrees respectively. For referring to unidirectional fiber, it will be used *Uni*.

The first step in determining the displacement, is to calculate the $[E]_{xy}$ matrix (equation 41), it represents the individual properties (table 4) for each material used in the sandwich panel, this means that each $[E]_{xy}$ will be different depending on the material and its orientation, the use of the matrix $[T]$, allows the use of different orientations for different plies is given by the equation 42.

$$
[E]_{xy} = \begin{bmatrix} \frac{1}{E_x} & -\frac{\vartheta_{yx}}{E_y} & 0 \\ -\frac{\vartheta_{xy}}{E_x} & \frac{1}{E_Y} & 0 \\ 0 & 0 & \frac{1}{G_{xy}} \end{bmatrix}
\tag{41}
$$

$$
[T] = \begin{bmatrix} C^2 & S^2 & -2C.S \\ S^2 & C^2 & 2C.S \\ C.S & -C.S & C^2 - S^2 \end{bmatrix}
\tag{42}
$$

The matrix $[D]_{ij}$ (equation 43), will result from the sum of the product between the matrix $[E]_{xy}$ and the height of the neutral line with respect to the referential axis as it can be seen in the figure 39.

$$[D]_{ij} = -\sum_{K=1}^{n} \bar{E}_{ij}^k \times \frac{Z_k^3 - Z_{k-1}^3}{3} \tag{43}$$
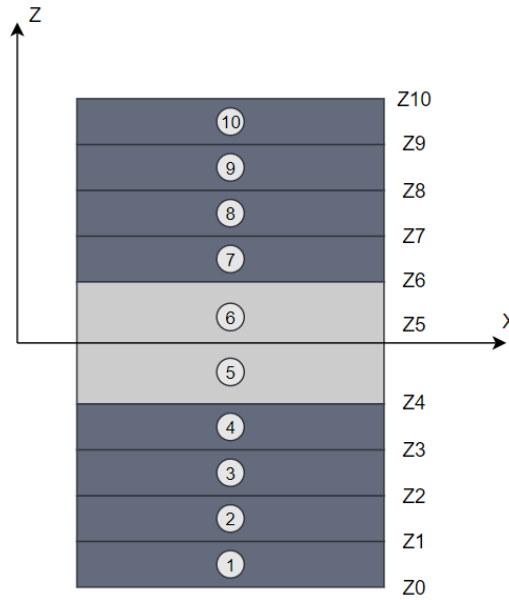

Figure 39: Example of a reference for the calculation of a laminate panel properties

After obtaining the matrix $[D]_{ij}$, that corresponds to the properties throughout the whole panel, through a simplification of the matrix $[ABD]$ (equation 40), the inverse matrix of $[D]_{ij}$ can be multiplied by the momentum´s vector, obtaining a vector, where the $\frac{\partial^2 w_0}{\partial x^2}$ will correspond to the deflection under the momentum M_x created by the force F.

Secondly, after obtaining a laminate that complies with the rules in terms of bending stiffness, the laminate was defined in a commercial finite element software, for this case it was ANSYS ACP, in order to confirm the results obtained between the theory and the finite elements, after confirming the panel has an equivalent EI to which steel tube or tubes the rules define.

Following the 3PBT, the PST simulations were made in order to guarantee that the laminate has not only the bending stiffness but also the shear strength defined in the rules for each panel. Since the result of a PST is a non-linear simulation, due to the fact that once the upper laminate fails, the panel will have a non-linear behavior due to it not having the complete properties that were defined at the beginning of the simulation. In order to get around this limitation, in Ansys it will be assumed that the upper and lower laminate fails once the failure criterion is equal and greater than 1, in all the plies of each laminate (upper and lower), in order to discover the two peaks of force during the simulation.

In order to simplify the understanding of the method used for the analysis, the figure 40 represents the methodology utilized for the analysis of each panel.
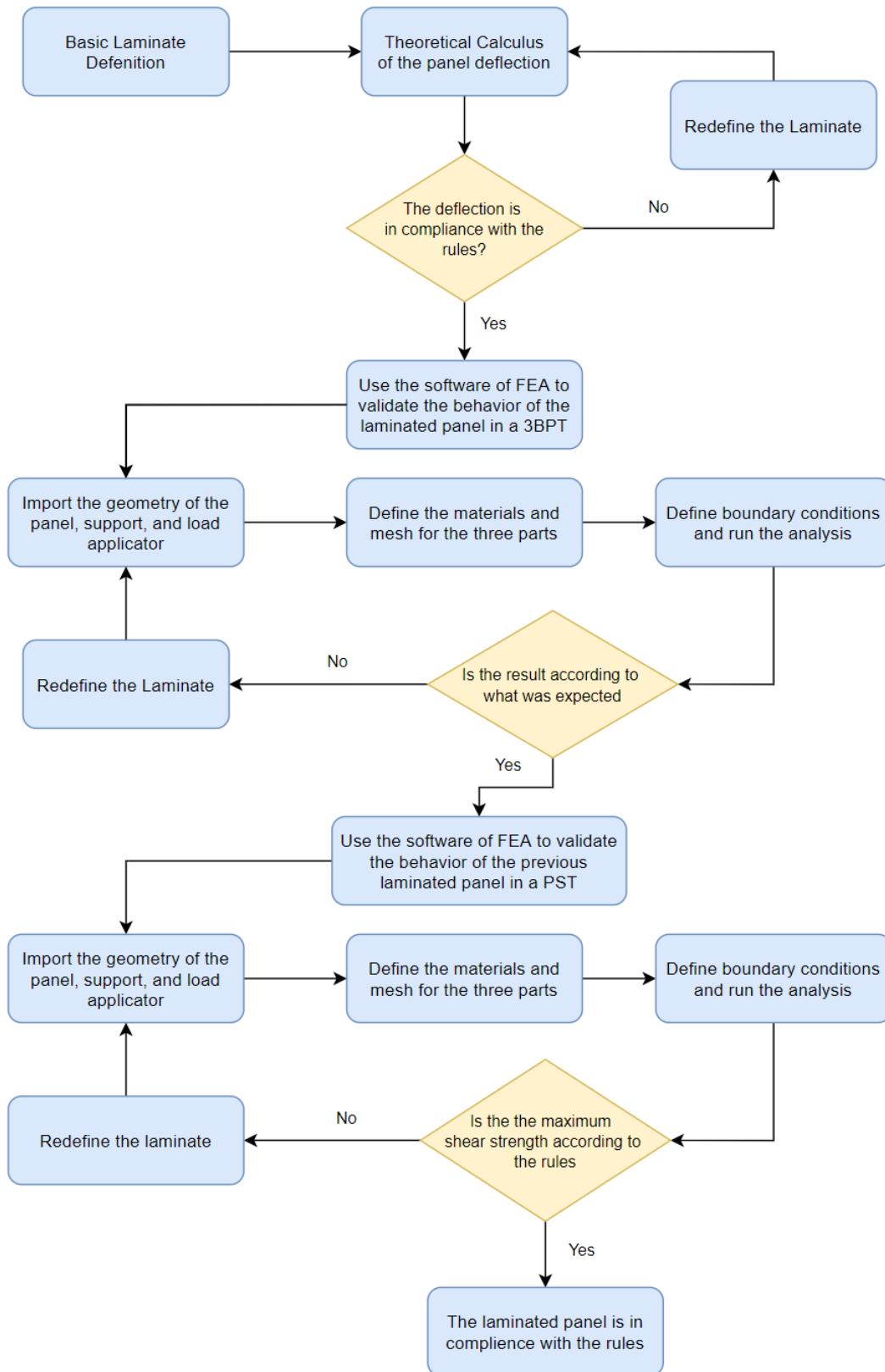
Figure 40: Working methodology represented on a flowchart

Table 4: Different material properties

Properties/ Material	Bidirectional Fabric (XC130)	Unidirectional Fabric (MTC510)	Aluminum Honeycomb
Density (Kgm^{-3})	1420	1490	2680
Thickness (*mm*)	0.25	0.286	10/ 15/ 20
Young´s Modulus X (*MPa*)	55200	119000	1
Young´s Modulus Y (*MPa*)	55200	8200	1
Young´s Modulus Z (*MPa*)	6900	8200	255
Poisson´s Ratio XY	0.04	0.01	0.49
Poisson´s Ratio YZ	0.3	0.34	0.001
Poisson´s Ratio XZ	0.3	0.01	0.001
Shear Modulus XY (*MPa*)	26358	59059	1E-6
Tensile Modulus X (*MPa*)	645	2282	0

3.3.2 *Defining the Analysis on a FE software*

A finite element analysis (FEA) software, is a computerized method for predicting how an object would react to real-world forces, vibration, fluid flow, and other physical effects, this type of analysis can predict if the object, that is being studied, will withstand the forces or will break, wear or not work the way it was designed for. The FEA is a very important step nowadays in developing new, strong, better parts for many different applications.

This type of analysis works by breaking down the geometry of the object in the study, into a large number of finite elements such as small hexahedrons, pyramids, wedges, etc..., like the ones in figure 41 Then through various mathematical equations, a computer will be able to predict the behavior of the object for the defined boundary conditions.
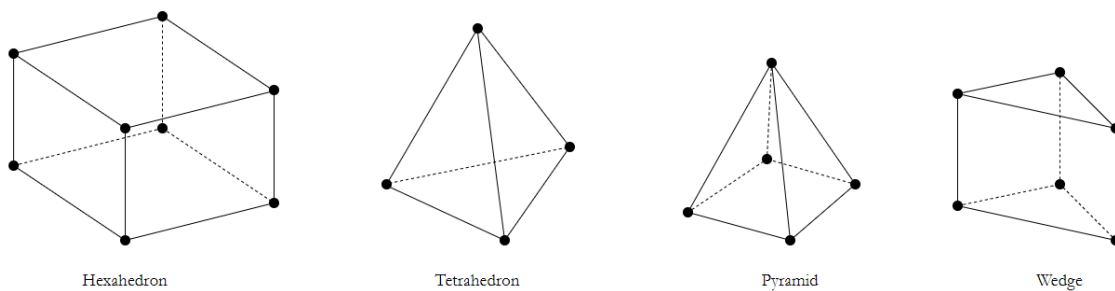

Hexahedron   Tetrahedron   Pyramid   Wedge

Figure 41: Different types of finite elements used in meshing

For the current study, this type of software allowed to perform the necessary simulations, as well as through the use of various failure criteria, such as the ones referred to in the section 2.1.4, to determine if the structure can or cannot withstand the efforts imposed on it.

There are many reasons for using a dual symmetry (figure 42) in a finite element analysis, such as the significant decrease in the number of elements present in the simulation.

That will allow using a finer mesh which translates into better and more realistic results in the analysis. Another reason is based on defining symmetrical solutions, since the problem is indeed symmetrical by two planes, the displacement of either faces present on either plane will only have displacement on the Y axis, this implies that per example the composite face where the symmetries plane is located will not have displacement on either the X or Z axis.
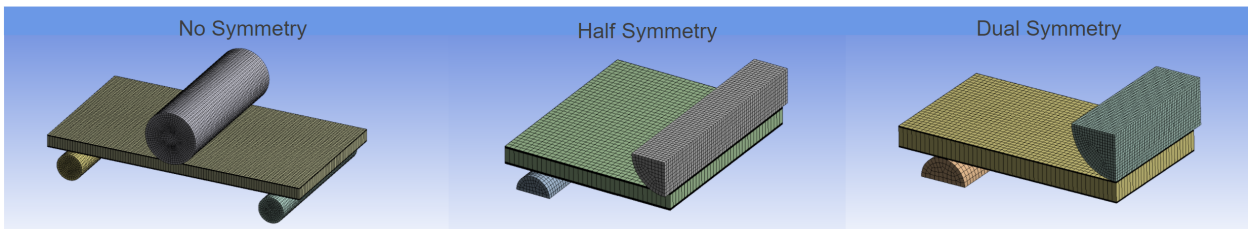

Figure 42: Different types of symmetries

For both analysis, Ansys used two different models from its database, *SOLID185* for the composite materials, and the *SOLID186* for the fixed supports and load applicator.

Through the figure 43 it can clearly be seen that the FE software uses different types of finite elements, like the ones mentioned above, to define the geometry of the three different objects present in this type of analysis. Both of the analysis contains around thirty thousand different elements in the mesh, this number may vary more or less depending on the number of layers present in the defined laminate. In order to get the most reliable results, the mesh was refined in the different points of contact, between the supports and the panel, and the load applicator and the panel.
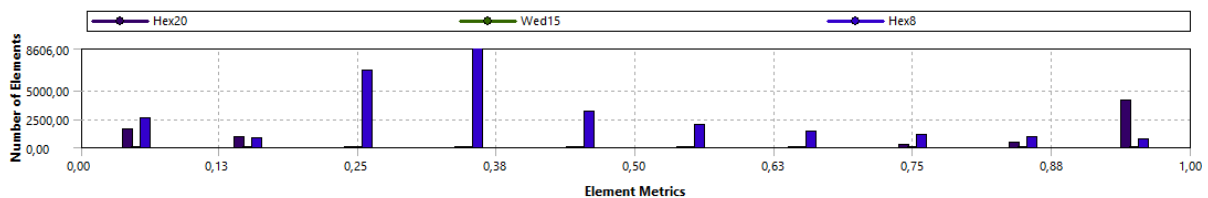
Figure 43: Different types of elements present in the mesh

The boundary conditions present in a 3PBT and the PST analysis can be seen in figures 44 and 45 respectively. Both contacts were defined to *frictionless* to allow for the sandwich panel to move freely to the force applied to the load applicator while being supported by the support.

Due to the dual symmetry in this analysis was necessary to define two *frictionless supports* in order to replicate the effect of symmetry in this analysis, there is also a *Remote displacement* so that the load applicator only moves in the Y-Axis, which was the direction where the load was being applied.

Figure 44: Boundary conditions for a 3PBT on FEA
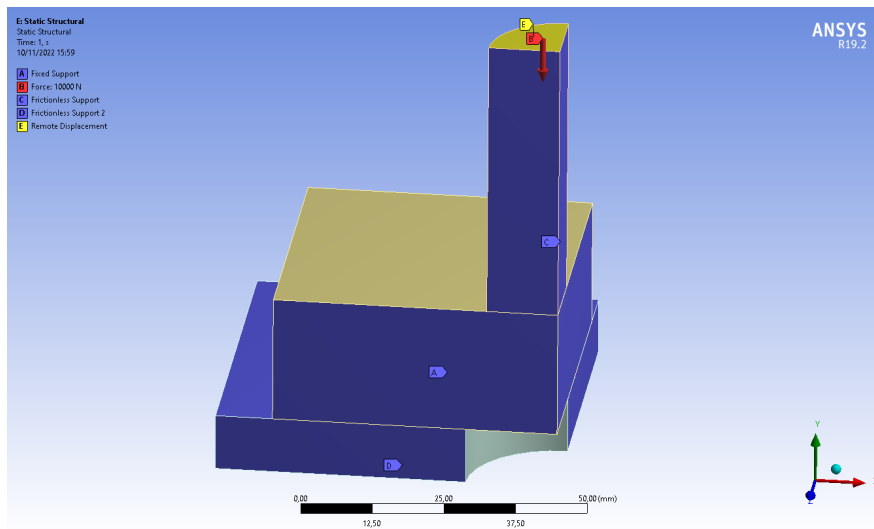
Figure 45: Boundary conditions for a PST on FEA

3.3.3 *Base Laminate Panel*

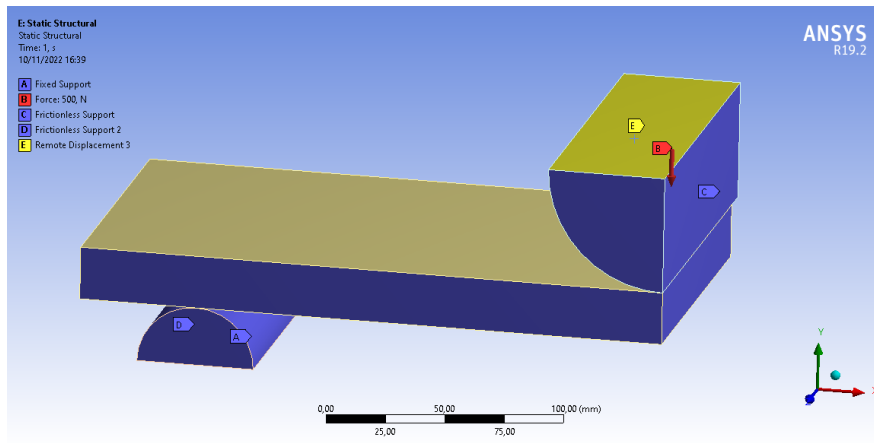For all other panels present in the monocoque, that are not mentioned within the rules, was used the base laminate already described above. The analysis results for this panel can be seen in table 6 and the laminate as well as the obtained *EI*. For this panel, it was also done a small study by varying the thickness (10, 15, and 20 millimeters) of the core including the flexural stiffness (table 5). The laminated used for this study was $[Bi_0/Bi_{45}/Bi_{-45}/Bi_0/Core]_s$.

Table 5: Core thickness comparison for 2000 Newtons and maximum supported force

Core (mm)	Theoretical Displacement (*mm*)	FEA Displacement (*mm*)	$EI(N.m^2)$	Failure Force (N)
10	3.81	3.71	724	3520
15	2.03	1.98	1370	5000
20	1.32	1.29	2120	6280

Through the results obtained (table 5), can be concluded that when using a thicker core, the higher flexural stiffness the panel is gonna have, this happens to the increase of the cross-section of the panel that results in a higher moment of inertia and also due to increasing the distance between the upper and lower laminates to the neutral line. For high flexural stiffness panels, it will be used the thicker core (20 millimeters), whereas in the other panels it will be used 10 or 15 millimeters honeycomb core in order to decrease the weight and overall size of the walls in the monocoque.

For the base panel, will be used the laminate present in table 6 with a core of 15 millimeters total since there is a decrease of 87% between 10 and 15 millimeters, and a difference of 35% between using a core with 15 millimeters relatively to thee 20 millimeters. While the analysis of this panel was being developed it was noticed that in the theoretical calculus the values obtained, in comparison thought the results obtained were constantly a hundred times smaller, for this reason on top of each value obtained by the theoretical calculus would be multiplied by hundred, this factor was also applied due to the access information of already tested sandwich panels, which was very close to the what was being obtained in the FEA.

Table 6: Base laminate FEA results

Lay-up	Theoretical Displacement (mm)	FEA Displacement (mm)
$[Bi_0/Bi_{45}/Bi_{-45}/Bi_0/Core_{7.5}]_s$	2.03	1.98

3.3.4 *Side Impact Structure*

Since this is a critical panel in the manufacturing of the monocoque, that must be in compliance with the rules, it is required to perform some tests in order to find out an adequate laminate that complies with the requirements (table 3). By using two different calculus spreadsheets, as the ones present in appendix B and C, it was possible to calculate a laminate that would comply with the flexural stiffness for each panel, using the equations shown above.

For the **vertical SIS**, the rules say that it needs to have a flexural stiffness as well as an absorbed energy equivalent to two baseline steel tubes and a perimeter shear strength equal to or bigger than 7500 Newtons, whereas for half of the **SIS floor** needs to have a flexural stiffness of one baseline steel tube.

Through the calculus spreadsheet, the laminate obtained for the vertical SIS can be seen in the table 7, by using this configuration as a baseline for the FEA, the simulation was performed on the finite element software, the results can be seen on the figure 46 and table 7, if a continues linear force would be applied it would be obtained an almost linear graph as the one present of the figure 47.

The absorbed energy from the steel tubes was calculated using data from experimental tests performed by another team [33].
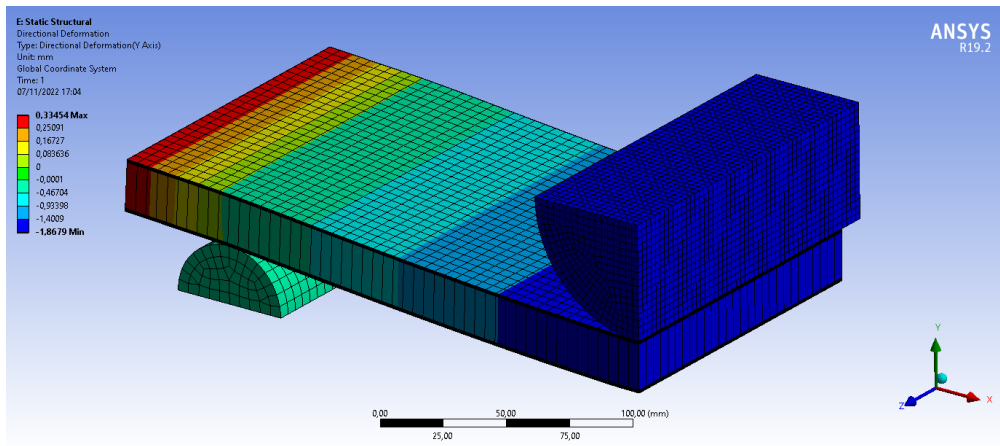
Figure 46: Vertical SIS 3PBT FEA: Displacement for a force of 4000 Newtons
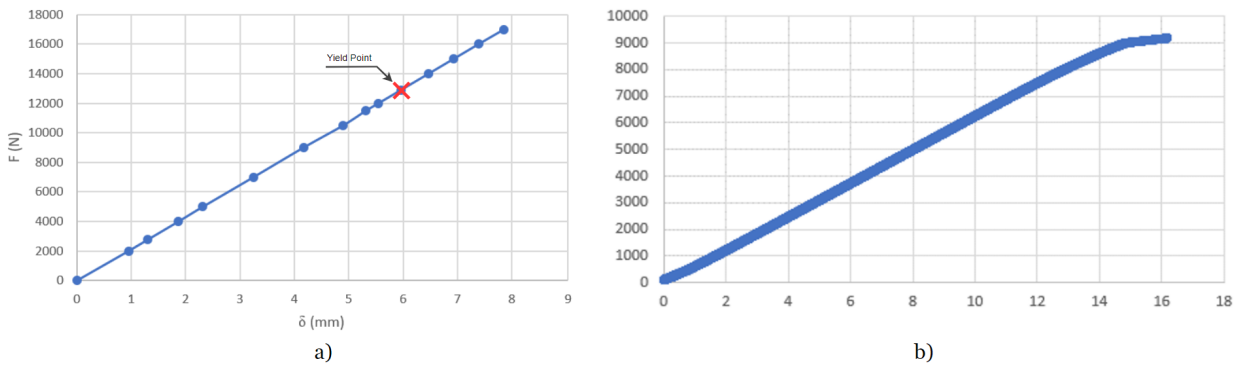

a)

b)

Figure 47: Force - Displacement graph: a) Vertical SIS 3PBT FEA results, b) Example, adapted from [33]

Table 7: Vertical SIS 3PBT results or a force of 2000 Newtons

	2x Baseline Tube 25.4 x 1.6	Theoretical	FEA
Material/Lay-up	Steel	$[Bi_0/Uni_0/Bi_{45}/Bi_{-45}/Bi_0/Core_{10}]_s$	
Displacement (mm)	12.7	0.97	0.95
$EI(N.m^2)$	3400	3705	3610
Absorbed Energy(J)	70.8	138.5	132.0

It can be seen that the difference between the theoretical results and the FEA is around 2%, some of the reasons for this difference can be the constraint definitions on the software and the way the finite element software solves the problem, another reason can be the fact that a theoretical calculus the force is being applied in a specific point whereas in the simulation the force is being applied through a cylinder load applicator as it can be seen in the figure 37.

Through the graph on figure 47 a) it can be seen that the maximum load until the panel fails is 12892 Newtons which is also higher than the ultimate strength of two baseline tubes (which is around 9000 Newtons according to the tests performed).

It can also be noticed that after the panel reaches its yielding point, in similarity with the test above, the behavior remains linear which would not happen in real life since the panel starts having a non-linear behavior (figure 47 b)). This means that despite Ansys recognizing that the laminate has reached its failure, it does not know how it will behave causing the graph to remain linear after the yield point, influencing directly in the absorbed energy of the laminate due to the increase of the area in the graph.

After the 3PBT analysis, the PST was performed in order to find the shear strength for the laminated sandwich panel defined above.
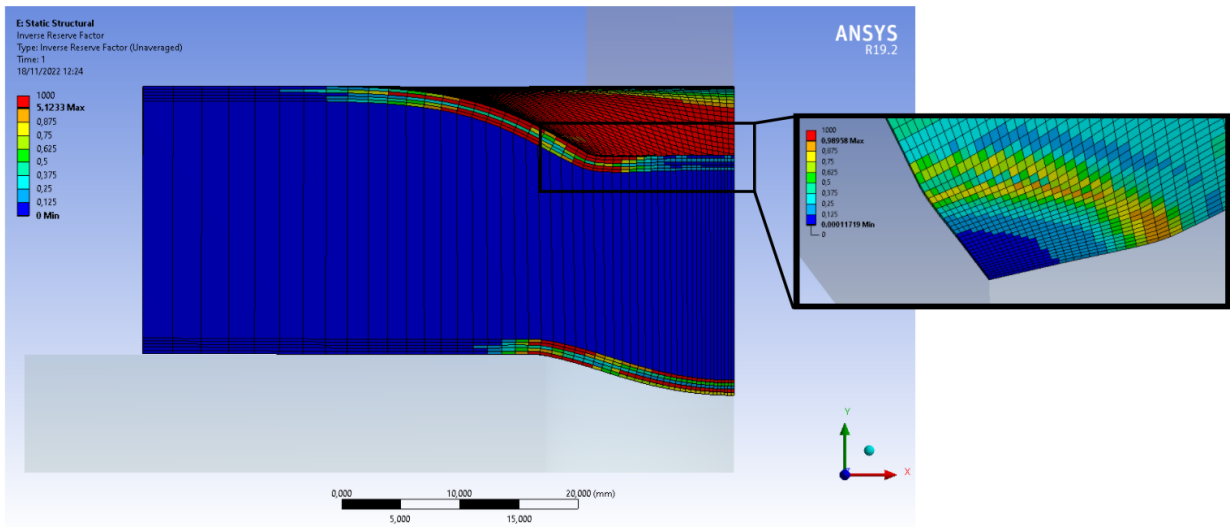

Figure 48: Vertical SIS PST FEA: Failure criteria for a ply at 45 degrees for 7500 Newtons

Table 8: Vertical SIS PST results

Laminated Sandwich Panel	Peak 1 (N)	Peak 2 (N)
$[Bi_0/Uni_0/Bi_{45}/Bi_{-45}/Bi_0/Core_{10}]_s$	7670	10480

Using the ANSYS mesh failure visualization tool for composite materials, the *Composite failure tool*, it is possible to observe whether the composite exceeds its structural capacity and goes into rupture or withstands the imposed load, through the value between 0 and 1, where 1 is the maximum value that the laminate can withstand before failure just like mentioned in the section 2.1.4.

In figure 48, it can be seen that despite the first ply in the laminate having a value greater than "1" the first peak does not occur until the upper laminate failed completely on all plies, through the use of this method, the second peak will occur while a higher force is being applied due to the honeycomb core contribution to the shear strength.

Throughout the PST FEA, it was noticed that the plies at "45" degrees would offer a greater shear strength in this type of analysis, in most cases being the last ply to encounter failure, in both the upper and the lower laminate as it can be seen in the figure 48.

Through the picture 49 and 50 can be seen the behavior of the panel when subjected to a shear force, it can be seen a "degrade" of color, with its origin in the edge of the load applicator where it is applying the force in the panel.
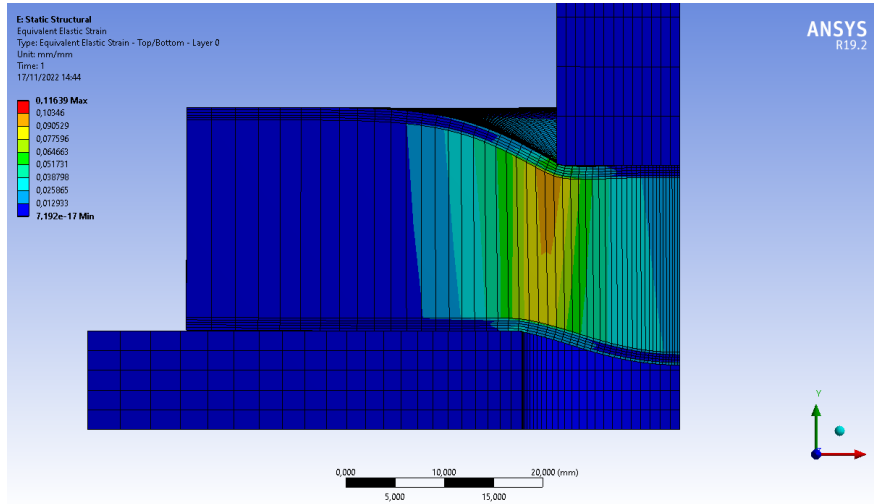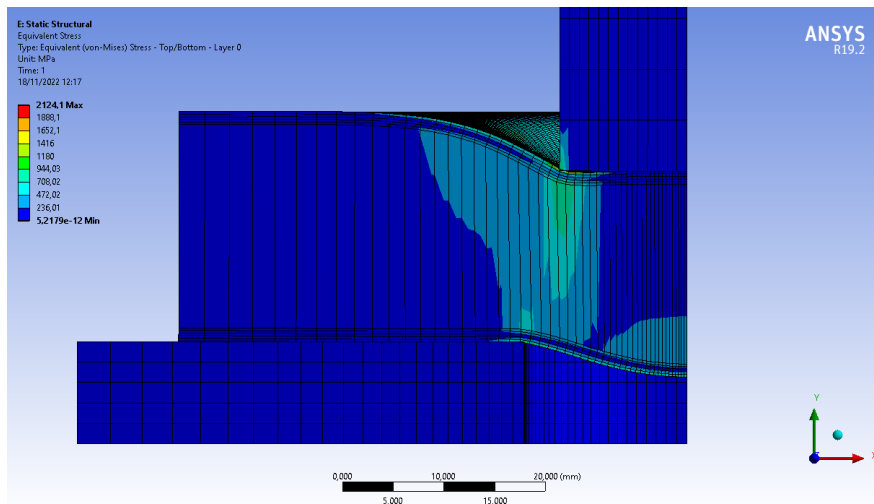

Figure 49: Vertical SIS PST FEA: Shear strain

Figure 50: Vertical SIS PST FEA: Shear stress

For half of the floor panel of the SIS, the analysis method was the same as above, since this panel is only required to be equivalent to one baseline steel it was used a thinner core of 15 millimeters in order to save weight and space.

In the beginning using only the base laminate and a core of 15 millimeters ($[Bi_\mathbf{o}/Bi_{45}/Bi_{-45}/Bi_\mathbf{o}/Core_{7.5}]_s$), the flexural stiffness was not in compliance with the rules, it was also used, in similarity to the vertical SIS panel, two plies of unidirectional fiber in the second ply in order to reinforce the laminate, the results for both before and after applying the reinforcing unidirectional fibers can be seen in the figure 51 and table 9.

From the table above can be seen that just by adding those two plies of unidirectional fiber, the panel obtained a flexural stiffness improvement of around 30%.
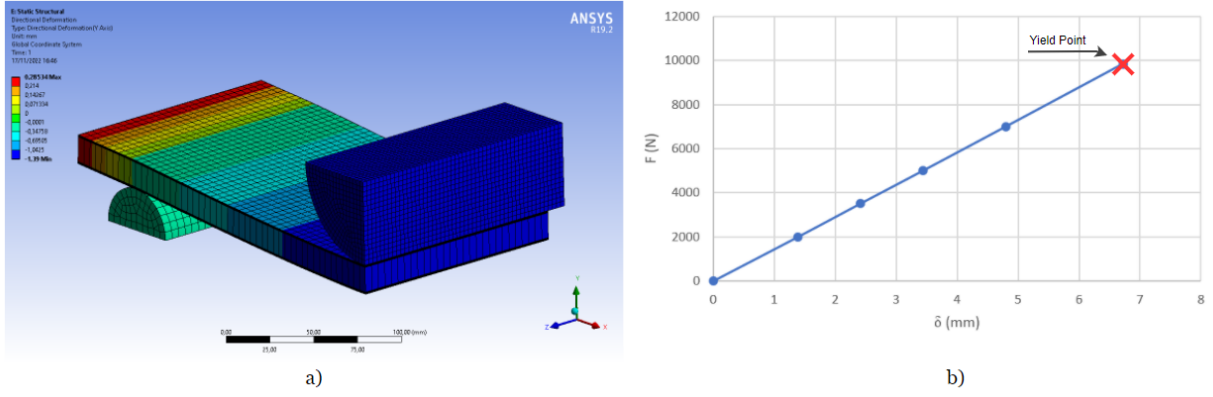
46

Figure 51: SIS Floor 3PBT FEA: a) Displacement for 2000 Newtons, b) Force - Displacement graph

Table 9: SIS Floor 3PBT results for a force of 2000 Newtons

	1x Baseline Tube 25.4 x 1.6	Without Uni Reinforcement	With Uni Reinforcement
Material/Lay-up	steel	$[Bi_o/Uni_o/Bi_{45}/Bi_{-45}/Bi_o/Core_{7.5}]_s$	
Theoretical Displacement (mm)	–	1.43	2.03
FEA Displacement (mm)	–	1.39	1.98
$EI(N.m^2)$	1700	1300	1950

From the results obtained for the vertical SIS as well as the floor, it can be concluded that, in theory, from the perspective of a finite element analysis, the laminate is in compliance with the rules presented in the table 3.

3.3.5 *Front Bulkhead*

Being this part one of the most important and crucial parts of the structure, since its where the impact attenuator (IA) and anti-intrusion plate (AIP) are fixed, elements of the vehicle that influence the safety of the driver in the case of a frontal collision, it also needs to be studied properly.

The SES provides a base value for the minimum perimeter shear strength of the sandwich panel for the front bulkhead, this value is equivalent to a 1.5 millimeters steel plate (table 3).

The shear stress and maximum stress strength of a composite panel as well as the perimeter shear strength are given by the equations 44, 45, and 46 respectively. Some of these equations were adapted in order to work in simple panels, this since SES makes a direct comparison of the values of the perimeter shear strength between the geometry of the front bulkhead, used in the monocoque, and the steel plate hence the high values.

$$\tau_{stress} = \frac{F_{Max}}{\pi.D.t}, \tag{44}$$

$$\sigma_{uts} = \frac{F_{Max}.l.(h+t_1+t_2)}{8.I_c}, \tag{45}$$

$$Perimeter\ Shear\ Strength = (W + L) * 0.002 * \sigma_{stress}.t_1, \tag{46}$$

Where:

- τ_{stress} = Shear Stress;

- D = Diameter of the load applicator = 25mm defined by the rules;

- t = Total Thickness of the panel;

- σ_{uts} = Maximum Stress Strength;

- l = Distance between supports;

- h = Thickness of the Core;

- t_1 = Thickness of the Upper/Outer Laminate ;

- t_2 = Thickness of the Lower Laminate;

- I_c = Moment of Inertia of the composite;

- W = Width of the composite panel = 100mm defined by the rules;

- L = Length of the composite panel = 100mm defined by the rules.

For the analysis of the front bulkhead, the starting point was the panel defined for the vertical SIS (7), since both needed to have an *EI* equivalent to two steel tubes, the main difference between the two comes to the perimeter shear strength of the FB being considerably higher than the Vertical SIS, due to its role in withstanding the absorbing force of the IA in case of a collision, for reference, for this panel size the PST has to be greater than 131000 Newtons, which is more than ten times the PST of the vertical SIS.

For the reinforcing of this panel were used multiple layers of mostly bi-directional fibers with different orientations in the outer laminate, but also with some unidirectional, in order to optimize not only the shear capabilities in the different directions but also the bending stiffness, by having many fibers in various orientations, the structure will have a higher shear strength.

The reinforcement plies used on this panel will only be applied on the outer laminate, this is due to the SES using only the thickness of the outer laminate to calculate the Perimeter Shear Strength of the FB, this will be the only laminate that will no be symmetrical through the center line, in this monocoque structure. The results of this analysis can be seen in the table 10.

For the front bulkhead bracing supports (FBHS) the laminate that will be used will be the same as the SIS floor (9) since, by the rules, both need to be equivalent to at least one steel tube, the main difference for the FBHS is that in total must have and equivalent *EI* of six steel tubes, which SES has pre-defined equations in order to determine if it is within the rules, by defining the area present in the monocoque, that this panel will be used. This panel also needed to have a PSS of 4000 Newtons which it has with a failure criteria factor of 0.61.

Table 10: Front bulkhead FEA results

Lay-up	$[Bi_0/Uni_0/Uni_{45}/Uni_{90}/Bi_0/Bi_{30}/Bi_{45}/Bi_{90}/Bi_{-45}/Uni_{45}/Uni_0$ $Bi_0/Core_{20}/Bi_0/Bi_{-45}/Bi_{45}/Uni_0/Bi_0/]$
$EI(N.m^2)$	5240
Perimeter Shear Strength (N)	133000 >131000 (Steel Plate)

3.3.6 *Suspension Attachment Points*

Despite not being in the rules how much the suspension points need to withstand, it is almost, if not as important as the other panels seen in the table 3.

Through the equations for the load calculations present in the subsection 2.5.4 above, and using a calculus spreadsheet (Appendix A) in *Excel*, for seven different scenarios, were obtained the following results presented in the table 11 and 12 for each individual arm (figure 52) both the front and rear suspension.

By observing the values obtained for the various scenarios, the maximum values of tension and compression to which each arm is subjected were obtained, as shown in the table 13, as is often the case the values in compression are negative and tension is positive.
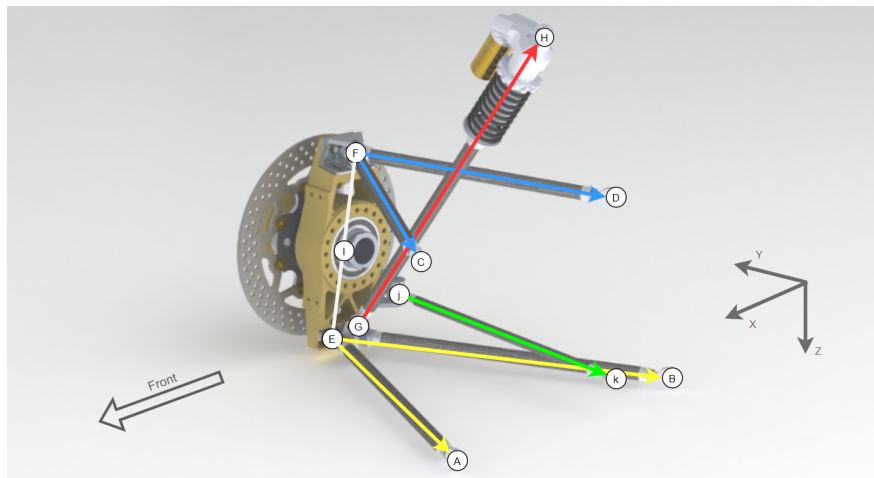

Figure 52: Suspension Arms Vectors

Before applying the forces to the laminated panel, was defined a safety factor (SF) that would be applied to the maximum forces that were obtained, the factor defined for this application was "1.5", which means that the part will fail at one and a half for the designed load, taking this into account, the force applied for tension and compression was around 11130 Newtons and 11165 Newtons respectively, in the motorsport industry, where a small reduction in weight has a great impact on the vehicle performance, is very common to see safety factors around "1.2", since the structure is made from composite materials and the manufacture would be made by students, due to being an FS competition, it was decided, for this case, to use an SF a little higher.

Table 11: Front suspension loads (N) for each individual arm

Vector	1.4 Left Corner	Left Corner Full Load Transfer	Braking 1.4g	Braking Full Load Transfer	Corner & Braking Combined	5g Bump	1.5g Vehicle Skid
EA	3323	3496	-359	-3246	1798	1440	1776
EB	2930	3081	2067	5718	3784	1111	1563
FC	136	139	2793	1578	2810	-164	12
FD	183	189	-2708	-1466	-2175	-82	37
JK	-7051	-7397	-876	-1238	-6156	-272	-3624
GH	-1197	-1273	-1134	-1618	-1283	-3812	-651

Table 12: Rear suspension loads (N) for each individual arm

Vector	1.4 Left Corner	Left Corner Full Load Transfer	Braking 1.4g	Braking Full Load Transfer	Corner & Braking Combined	5g Bump	1.5g Vehicle Skid
EA	521	549	-1145	-4448	-767	185	305
EB	-7245	-7443	-164	2190	-5537	-2094	-3629
FC	175	186	3752	2282	3469	714	79
FD	-463	-476	-1885	-434	-2383	2793	-278
JK	7443	7320	1658	2396	6779	2874	3792
GH	-2186	-2315	-1415	-2014	-2129	-4499	-1180

Table 13: Maximum suspension loads (N) for each individual arm

Vector	Front		Rear	
	Compression	Tension	Compression	Tension
EA	-3246	3496	-4448	549
EB	-2930	5718	-7206	2190
FC	-164	2810	-2282	3752
FD	-2175	189	-2383	2793
JK	-7051	7051	-7443	7420
GH	-3812	1197	-4499	2186

As already mentioned above (section 3.2.3), in the suspension points, will be used aluminum inserts, due to its high compressive strength. Due to this analysis having two different compositions in one geometry its necessary to use the tool "named selection" in order to select the two different zones with different laminates.

The laminate with the aluminum honeycomb and the other with the aluminum insert, can be seen in the figure 53 a).

For this analysis was used a common rig (figure 54) for testing tension and compression in composite panels, it uses two steel plates in order to lock the sandwich in place, both in a whole in a middle to allow deflection in the Y-Axis for both sides.
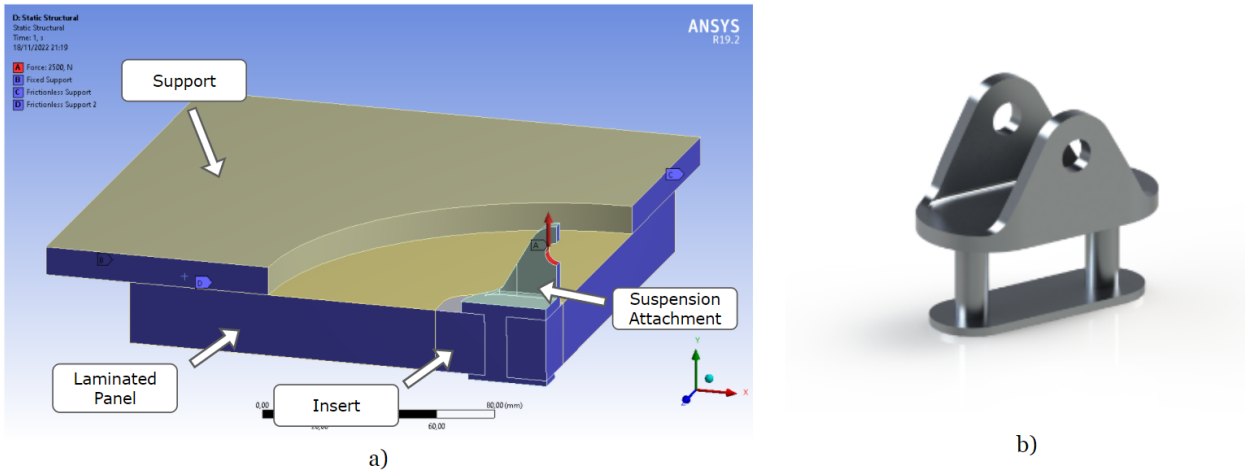
Figure 53: Suspension attachment point FEA: a) Boundary conditions, b) Suspension attachment part

In this FEA the whole will be around 200 millimeters in diameter, in the figure 53 b) can be seen that the suspension attachment point used in the analysis already has the bolts and backing plate Incorporated in the geometry that will be imported into the finite element software.
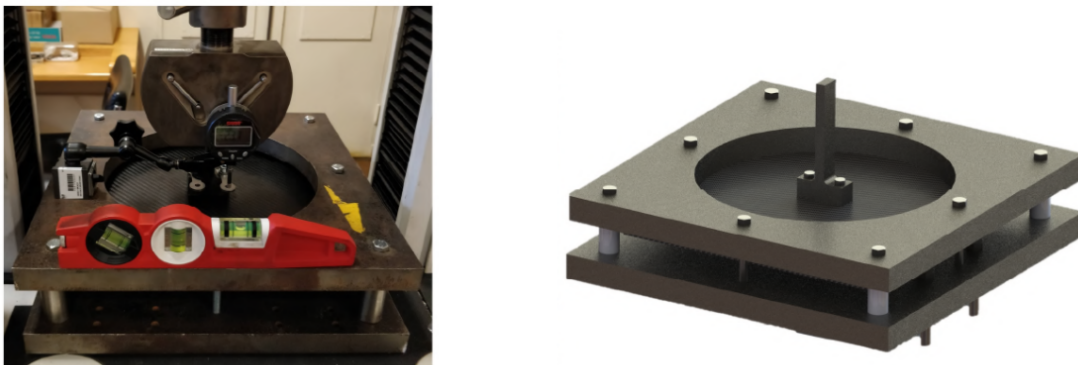

Figure 54: Insert testing rig, adapted from [29]

The first analysis performed was with the force of 11130 Newtons (traction force) on the suspensions attachment point, this value was chosen, as mentioned above to have a safety margin due to the method used for the force calculation and in case there is a peak force during an awkward situation, the laminate was "bonded" to the steel structure above in order to secure the laminate in place during the analysis, the suspension point attachment part is also "bonded" as it would if it was secured by the bolts.

For the compression analysis of the laminate with the insert, it was used the same conditions as above but instead of using a positive value for the force, the load applied was -11165 Newtons. The results for both can be seen below:

Table 14: Laminate used in the suspension points

$$[Bi_0/Uni_0/Uni_{45}/Uni_{90}/Uni_{45}/Bi_0/Bi_{45}/Bi_{90}/Bi_{-45}/Bi_{45}/Bi_0/Bi_{45}/Uni_{45}/Uni_0/Bi_0/Core_5]_s$$
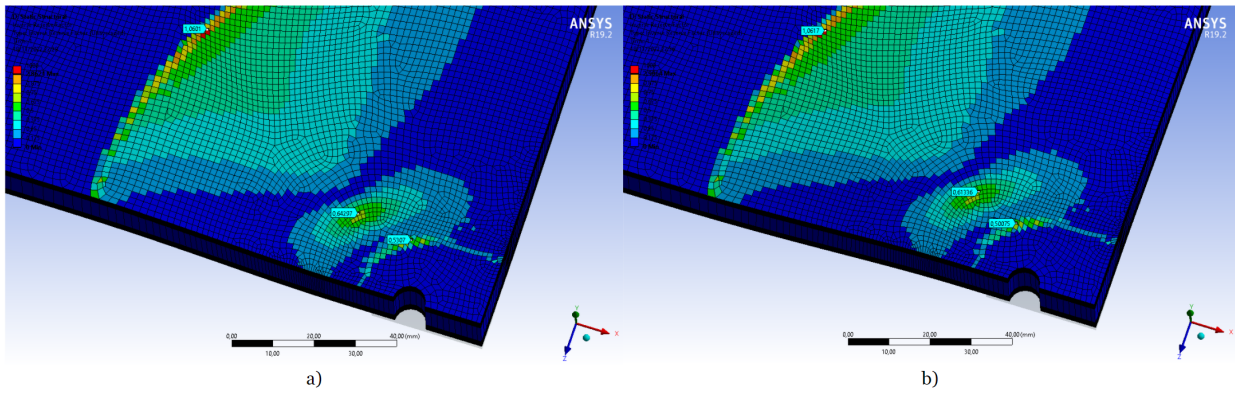
Figure 55: FAE results on suspension attachment point: a) Compression, b) Tension

It can be seen, through the results shown above, that by applying both a tension and a compression force on the suspension attachment point the point of failure starts where the panel is being attached (figure 55), while the zone where the insert is located still have not reached failure.

The displacement present in both analysis is minimal taking into consideration the enormous force being applied to the panel obtaining values of the deformation on the Y-Axis around one millimeter maximum, the final laminate that will be used on the suspension panels can be seen in the table 14 above.

3.4 DEVELOPMENT AND STRUCTURAL ANALYSIS OF THE MONOCOQUE

For the development of the monocoque geometry, was used SolidWorks, a Computer-Aided Design (CAD) software allows the creation of surfaces that will give shape to the outside shell of the monocoque.

Through the various tools, featured in this software, it is possible to design the desired structure. The design has undergone several iterations, which can be seen in the figure 56. In order to achieve a design that complies with the regulation, and that all components intended to be incorporated into the vehicle fit with some margin, so that both the cooling lines as well as the electrical auxiliary parts have the necessary space to be mounted.

In figure 57 can be seen some of the representative volumes for some of the components that make up the tractive system (TS) like the accumulator, electric motors, and inverter present in the section 3.1.3, also in the picture are present both hoop (front and main) in order to know where the supports for them are located in the monocoque.

A geometry surface based was imported to Ansys ACP pre module, which is responsible for defining and simulating composites materials only works with surfaces and not solids. This module only recognizes surfaces due to limitations.

If the geometry of the monocoque was imported as a solid it would have to be converted into a surface inside the software, this method was also used in the study of the sandwich panels studied above.

First Iteration   Last Iteration
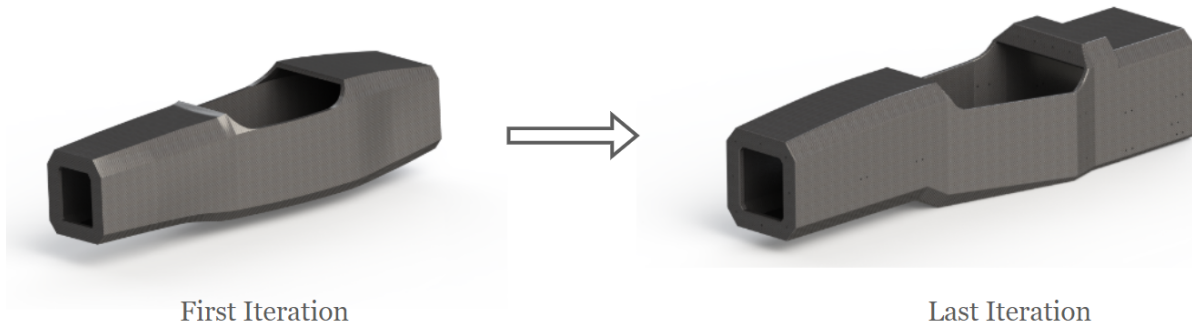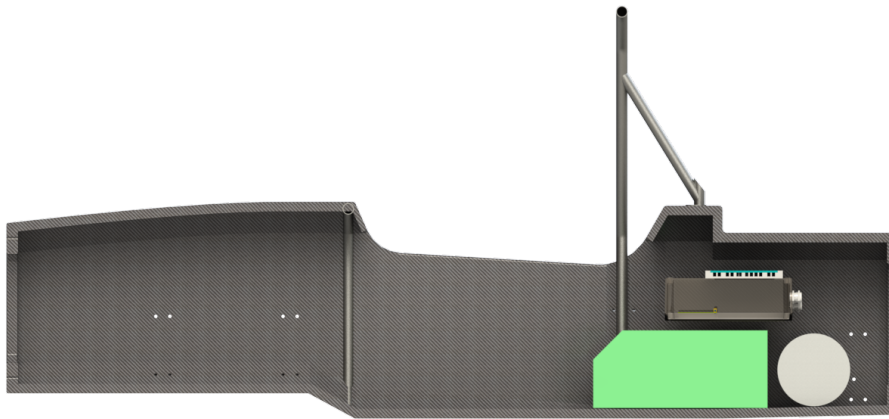
Figure 56: Monocoque geometry evolution

Figure 57: Monocoque split view with both hoops, battery, motor, and inverter

For the creation of the mesh, it was necessary to define the maximum size that each element can have, this is necessary in order to ensure that the mesh has enough definition to cover all the details present in the structure, in this case, the maximum element defined was fifteen millimeters, due to most of the surfaces present in the geometry are big panels.

For the more complex zones like holes or small fillets Ansys automatically refines the mesh, in order to have more accurate in critical places, like the zones where inserts are used, it was a manual meshing size tool to refine the mesh even more.

The mesh of the exterior surface is represented in the figure 58, for the analysis of the full structure, the number of elements in the total was around 69534 elements.

As there are many different zones that need to be defined individually, as already made above in the suspension analysis due to the use of inserts, to use the tool "named selections" in order to select the various different zones with the different laminates, can be seen in the figure 59. Due to the use of various panels, there will be various thicknesses as well as properties along the monocoque structure, as can be seen in the lateral of the caption different colors correspond to different thicknesses.
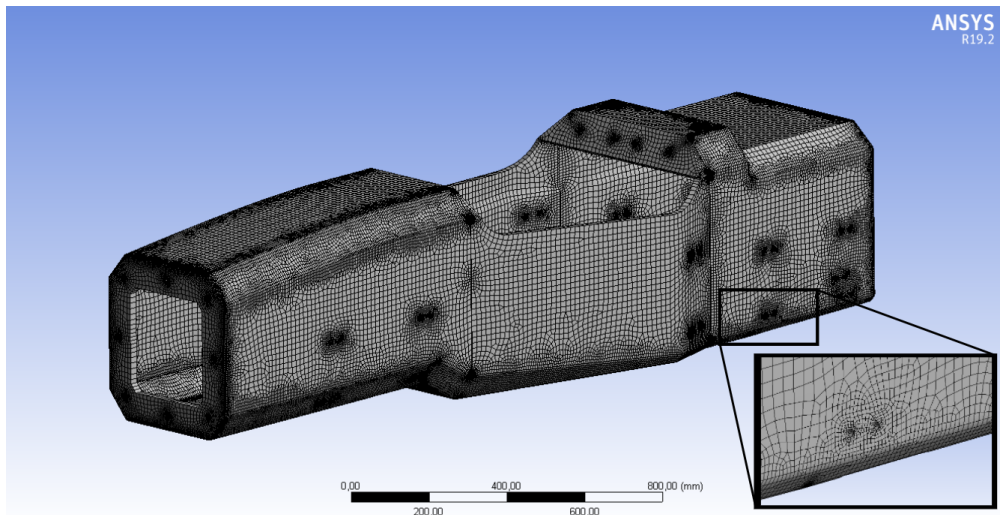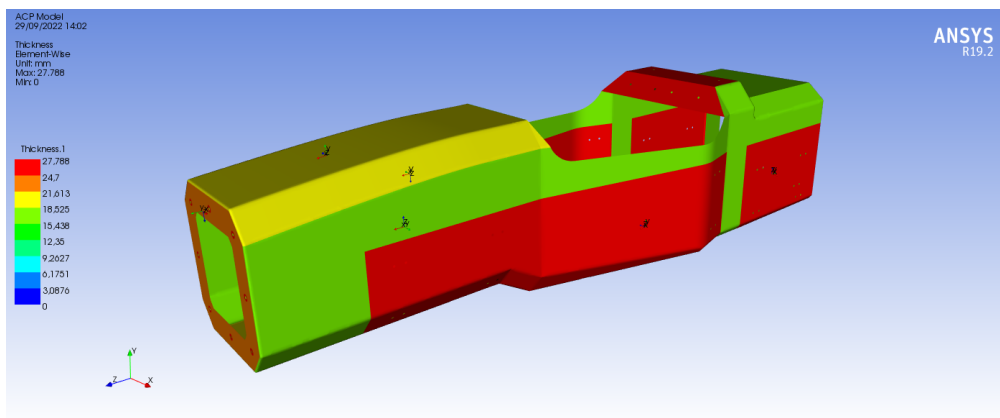
Figure 58: Monocoque mesh

Figure 59: Different panels thicknesses present on the monocoque

In order to define all the different panel properties and lay-ups, different "oriented selections" need to be defined, as well different "modeling groups" (figure 60).
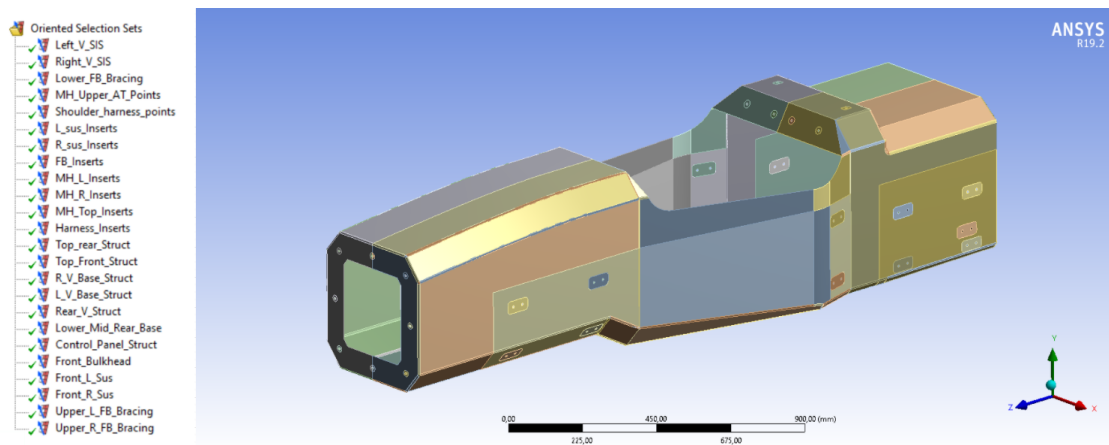

Figure 60: Different surfaces present on the monocoque

After having the structure of the monocoque all defined, the full structural analysis of the monocoque could be started, this analysis will be divided into two distinct parts, the first one will

be a structural study through the use and application of the suspension loads applied on the outer shell of the monocoque, the second one will be a torsional stiffness study in order to compare the results to a conventional steel space frame chassis.

3.4.1 *Suspension Loads on the Monocoque Shell*

For the analysis of the suspension loads applied to the outer monocoque shell, will be used the loads for the various dynamic conditions presented above in the section 3.3.6. In the analysis of the front suspension forces, the loads were applied in the insert where the attachment points would be placed, while the rear attachment points were fixed as can be seen in the figure 61 a), for the rear suspension analysis was used the same method but instead of applying the forces in the front attachment points, these were applied on the rear while fixing the front (figure 61 b)).

For both this analysis were not used the suspensions attachment part that used in the 3.3.6 due to the complexity of introducing contacts between the solid parts and the composite structure, this would greatly increase the level of complexity of the FEA as well as the time required to run the analysis.

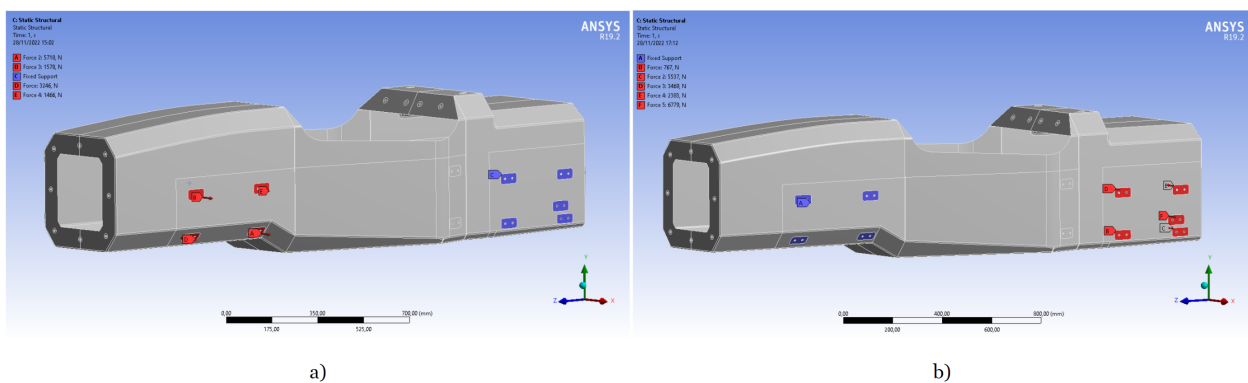a)   b)

Figure 61: Monocoque FEA suspension loads boundary conditions: a) Front, b) Rear

Through the different dynamic scenarios loads, can be seen that, despite having analyzed the suspension panel individually above, it can be clearly seen that the geometry of the monocoque in specific areas plays a big role in the structural integrity of the monocoque, in the case of the front suspension, there is a zone that reaches failure, due to the steep angle of transition between the two geometries and lack of *"fillet"* in that zone, there is a stress build-up which led to the failure of the laminate as it can be seen in figure 62.

In order to solve this design flaw in the front of the monocoque structure, were applied two plies of bidirectional fiber at [0/45] degrees angle on each (inner and outer) laminate, which solved the failure for the suspension loads.

Another solution could have been to change the geometry of that specific area so that the transition would not be so aggressive. By applying the reinforcement in that area was noticed a reduction of 6 % in the stress.
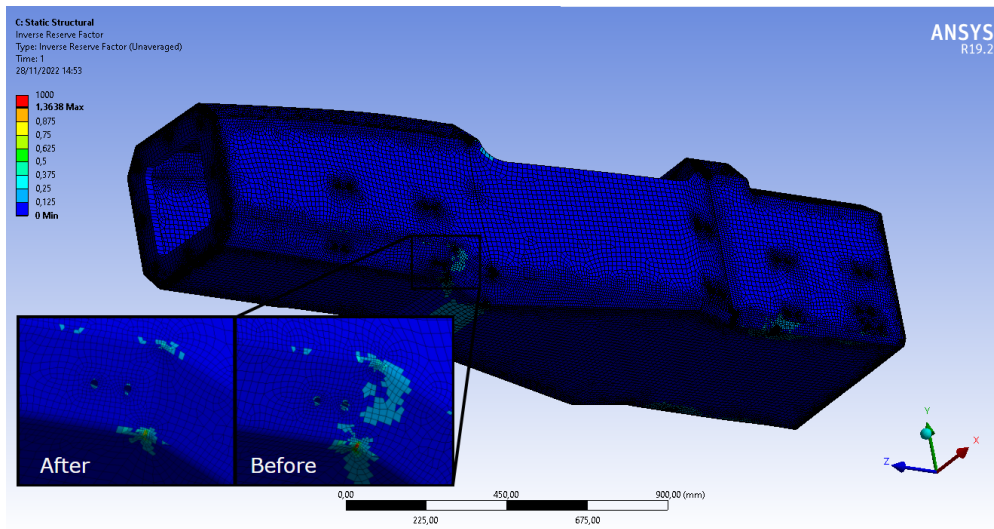
Figure 62: Mono FEA: Failure zone in the front suspension attachment before and after reinforcement

In the analysis of the rear suspension was noticed that, due to having a small area for the force to be distributed, in specific, where the lower A-Arm suspension attachment points are, there would also be stress built up in the rearmost support, as can be seen in the figure 63.

In order to reinforce this area were used four bidirectional fibers plies at [0/45/90/0] degrees in both laminates. After it was applied the reinforcement and noticed a reduction of 17 % in the stress of the maximum point in that area.
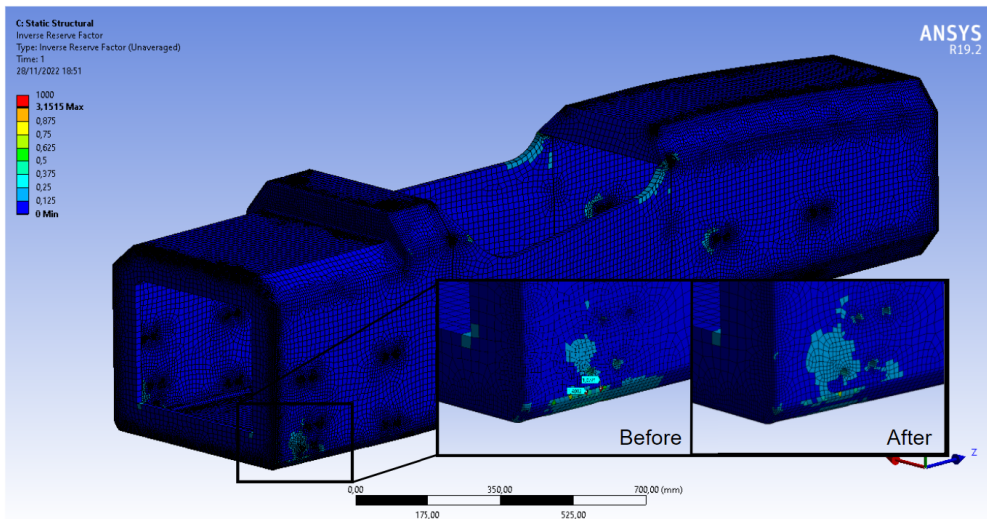

Figure 63: Mono FEA: Failure zone in the rear suspension attachment before and after reinforcement

For both, the front and rear suspension analysis, the maximum obtained deflection was less than one millimeter after applying the reinforcement which is a difference of 19% in the front and 42% in the rear attachment points.

After reinforcing the zones located around the suspension points, critical failure zone continued to appear where it was already expected. This is the zone where there is a steep transition between the middle and the front of the monocoque, where the front hoop would be located inside the structure in order to reinforce it.

In similarity to what was done above on the suspensions points, there are two solutions, either reinforce that zone or modify the geometry around that area to prevent stress build-up in the edge as seen in the figure 64 or the geometry is modified to allow a smoother transition between the two parts of the structure.
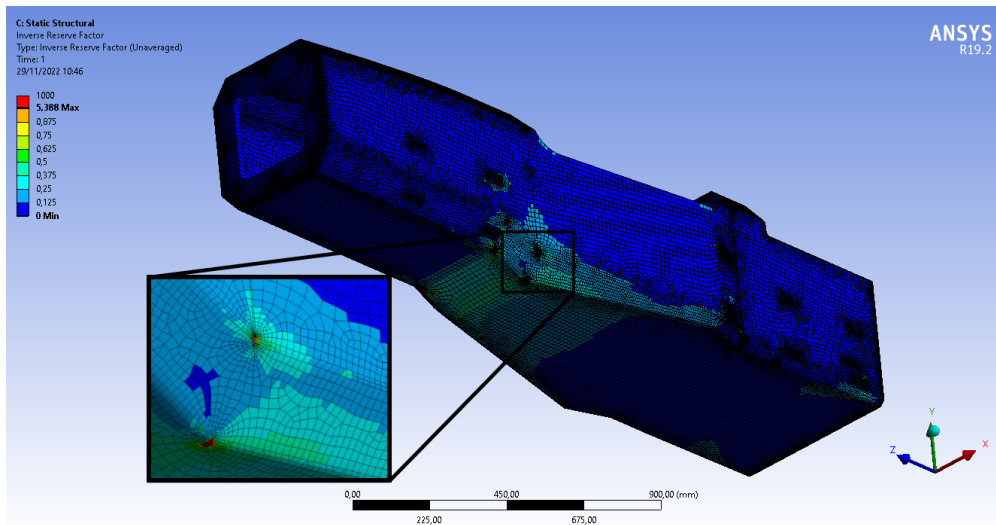

Figure 64: Mono FEA: Failure in the most critical zone

In this analysis (figure 64), despite trying to reinforce the structure in that specific area with various carbon fiber plies in both laminate, the failure in the laminate would still appear due to the geometry flaw, although modifying and redesigning the geometry of the monocoque being a better solution. This process is very time-consuming due to the complex shapes present in the CAD model, as well as, redefining all the different zones of the monocoque in the finite element analysis software.

3.4.2 *Torsional Stiffness and Comparison to a Conventional Space Frame Chassis*

For the torsional stiffness analysis, the boundary conditions (figure 65) in this analysis were quite simple, as already shown above in the figure 10 in the section 2.4.

Two forces were applied on opposite sides in the upper frontmost suspension attachment points since these points were located near the center line in the monocoque, while securing the rearmost attachment points, this in order to create a torsional momentum that will translate into a small displacement in the Y axis that will be used to calculate the torsional stiffness of the monocoque.

This type of analysis is independent of the force being applied in the structure, due to the displacement being directly proportional to the applied force. For this analysis the force being applied was 1500 Newtons. The results obtained for the monocoque torsion analysis are present in figure 66.

In order to have a direct comparison to a space frame chassis, were used the properties of the previous formula student vehicle from FSIPLeiria, the T22, the torsional stiffness analysis on the tubular chassis can also be seen in the figure 67. The final comparison results are present in the table 15.
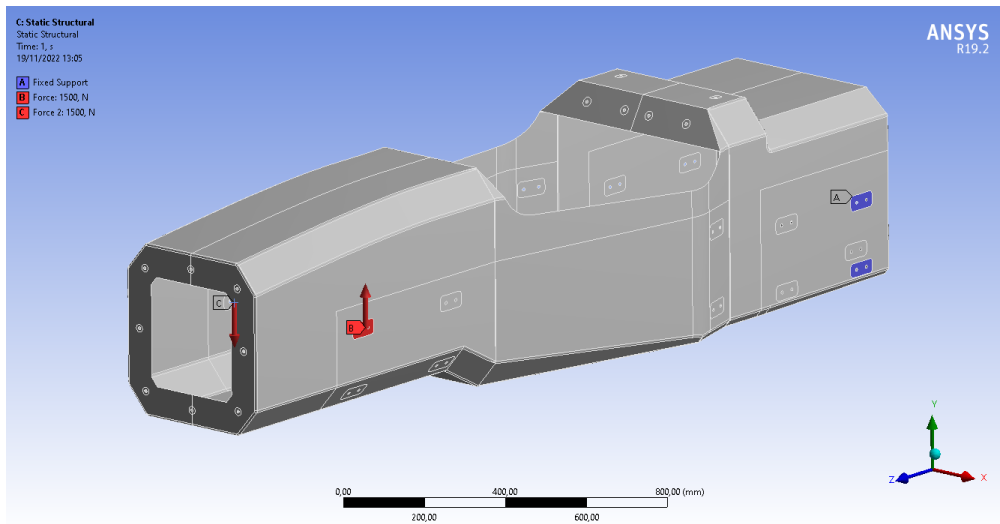
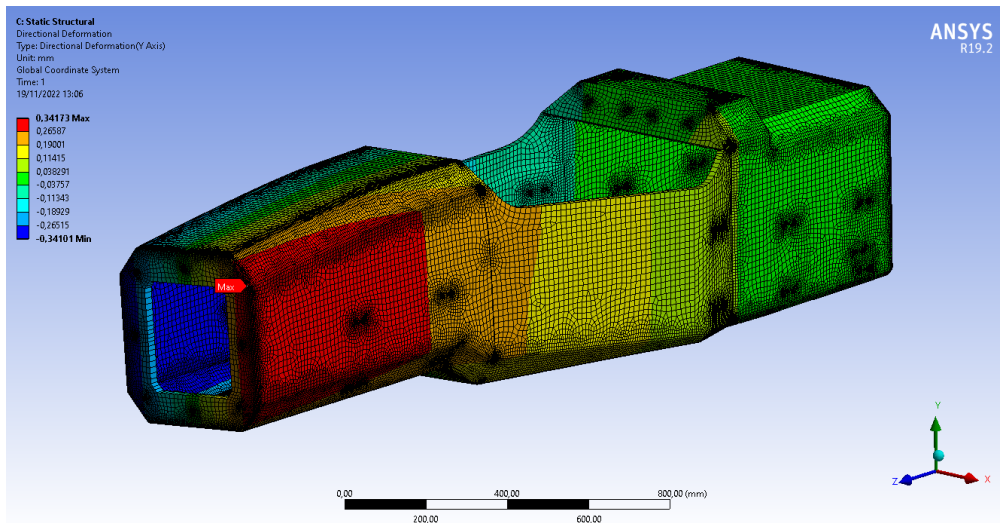Figure 65: Mono FEA: Torsional stiffness boundary conditions

Figure 66: Mono FEA: Displacement on the Y axis on torsion momentum
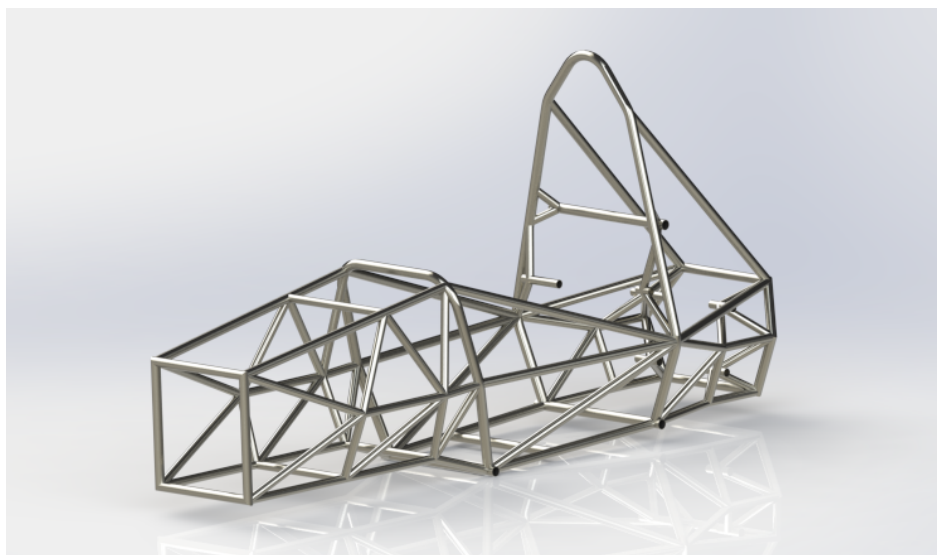

Figure 67: Space Frame Chassis - FSIPLeiria T22, adapted from [34]

Table 15: Comparison between space frame and monocoque for a force of 1500 Newtons

Properties/ Chassis	Space Frame [34]	Monocoque
Material	Steel	Sandwich Carbon fiber Panels
Displacement (*mm*)	2.23	0.34
Torsional Stiffness (*Nm/degree*)	1992	21345
Weigth(*Kg*)	37.3	55.4

By comparing the results between the two types of chassis, in particular the weight, can be seen that the monocoque after all the analysis and the reinforcements placed in the critical zones was around 32% heavier than the previous chassis, which was already expected since the panels of its structure are not optimized.

One option to save weight in specific zones is where the stress builds up due to the complex monocoque geometry, smaller shaped reinforcements can be applied instead of adding an entire new ply to the whole panel.

The use of geometry optimized and another type of materials for the inserts instead of only using aluminum contributes to a big weight saving due to the numerous inserts that need to be used in this type of structure.

The monocoque chassis, as expected, offers a greater torsional stiffness due to the high strength, stiffness, and area of the sandwich panels. The difference between both chassis was more than ten times.

Through the use of topology optimization software, the structure can be optimized for specific cases, this type of software usually runs the various scenarios while rearranging the different plies or even removing them while not compromising the structural integrity of the structure, this will contribute to weight saving while maintaining the overall strength and stiffness.

In conclusion, this structure can still be very optimized, not only through the use of different inserts and plies configurations but also in its geometry to allow a better stress distribution and smoother surfaces.

MANUFACTURING PROCESS

The whole process of manufacturing a monocoque chassis is difficult and delicate due to its complexity, and the attention to detail, required in order to achieve structure with an overall good outer surface finish, but even more important, a structure with good mechanical behaviour.

4.1 MOLDS FOR THE MONOCOQUE

4.1.1 *Positive/ Male Mold*

For the Manufacturing process, it is necessary to start by designing the necessary molds in CAD, so that later they can be machined from medium-density fibreboard (MDF) blocks, preferably one that provides a good surface finish after being machined and is not very porous, or from a high-density foam such as Necuron. In this case, is needed two positive molds like the ones in the figure 68 below.

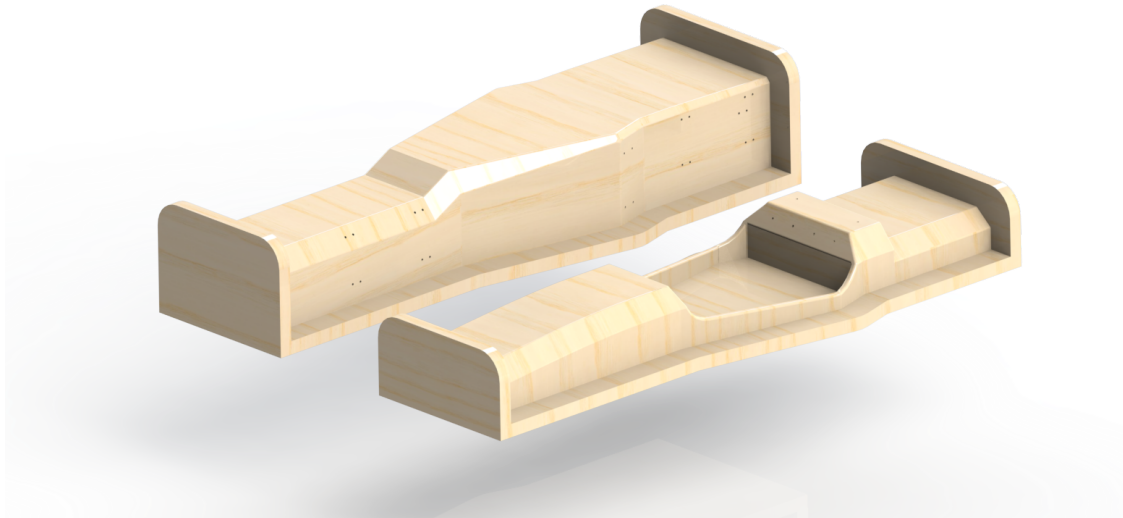Figure 68: Monocoque positive mold

The purpose of producing the molds, shown above, is to laminate the negative mold that will be used for the production of the monocoque itself over the one that was machined. These will be machined on a computerized numerical control (CNC) machine suitable for machining large, porous materials to accommodate the large dimensions of the molds as shown in figure 69.

Figure 69: Example of a monocoque positive mold being machined with a CNC, adapted from [35]

After machining the two molds, it is necessary to finish the surface by sanding them with sandpaper of different grids in order to achieve a surface without imperfections and then applying a gel-coat resin to leave the surface with no imperfections with a gloss finish, this surface is gonna play a major role in the finish of the final monocoque surface.

4.1.2 *Negative/ Female Mold*

This mold will be created, as mentioned above, from the positive mold (figure 68), for the lamination process it is not required to use carbon fiber, however, the use of carbon fiber with the same thermal properties as the fiber that will be used in the monocoque, will provide a better overall surface finish and have the same deformation thermal properties (contraction and expansion) when the mold goes onto the autoclave to cure the laminate. The process used in the creation of these molds can be a conventional, more affordable process, such as a wet-layup, instead of the use of pre-impregnated fibers, which are very expensive. During all the lamination processes, just like it was considered in the structural study above, the zero degree orientation that will be used is from the back to the front of the mold, in the longitudinal direction as shown in figure 70.

After the lamination process, it can be removed from each positive mold, the new negative mold will be attached to the other negative mold from the bottom together with two plates (a front and a back one), one in the front and one in the back, as in figure 71, with everything locked together it can then be started the lamination process of the monocoque itself present in the next section.
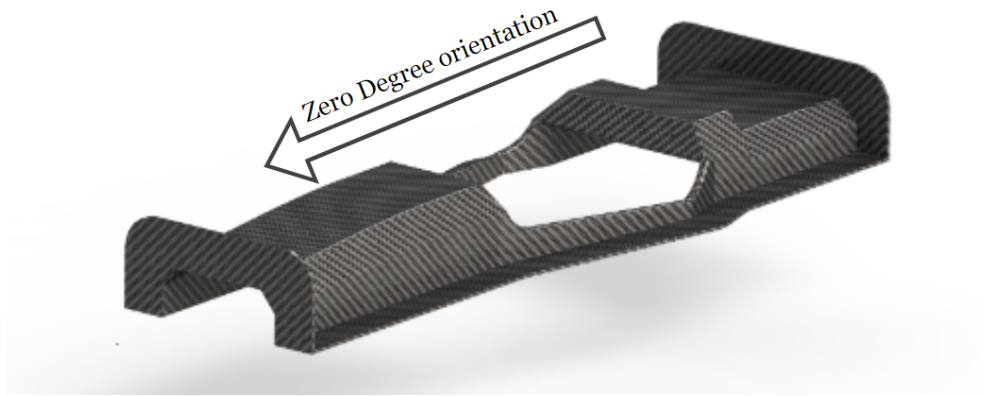
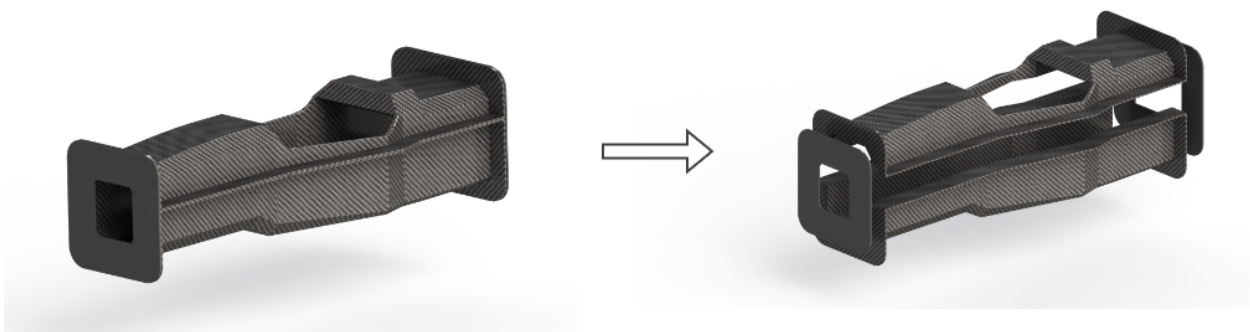Figure 70: Top negative mold of monocoque with fiber orientation

Figure 71: Assembly of all the negative molds with front and back plates

4.2 PRODUCTION PHASE

This process will consist of three curing phases, the first one, where the outer layer of the monocoque will be placed all around the monocoque, in order to cover the entire exterior surface of the monocoque, you have to be very careful in placing this layer as it will be the aesthetic layer that you will see, the second one will be the lamination of the main hoop that, by regulation has to be integrated inside the structure, where the top layer of it has to be locked behind the core of the structure around it. The third and last is the placement of the adhesive between the core and the fiber, the core or inserts, and the last layers of fiber.

It is very important while cutting the honeycomb for the core to cut it at the determined angle in order to allow the junction between the two cores to be as perfect as it can be or it will have a small space inside the structure that will not have a core inside which will weaken the structure that can cause failure in the laminated panels in that zone, is also as important to have this attention while cutting the wholes on the honeycomb for the inserts to be placed inside (figure 72 a)) .

Since this is an electric vehicle, after all the lamination process is finished, a copper mesh will have to be applied (figure 72 b)) in order to make mass points, since it is not a tubular chassis there is no mass of the chassis itself, so the mesh will immolate that effect, one of the other advantages of using this mesh, is the galvanic reduction of the aluminum, which is generated by the passage of currents through it, which is found both in the core and in some inserts of the monocoque, thus increasing the mechanical strength and longevity of the structure.
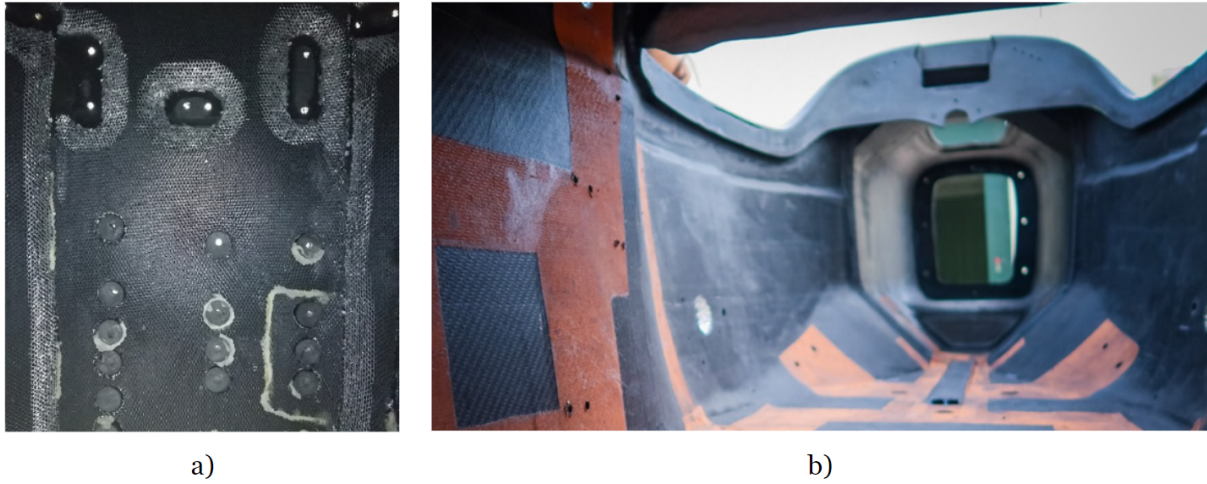

a)   b)

Figure 72: a) Inserts on Honeycomb, b) Copper mesh in the monocoque panels, both adapted from [35]

CONCLUSION AND FUTURE WORK

5.1 FINAL CONCLUSIONS

The main objective of the current project was to design and develop a full carbon fiber monocoque for a formula student electric vehicle belonging to FSIPLeiria team. This project also serves as a way to enhance even further the team's knowledge in this area.

Based on finite element analysis, different panels integrated in the monocoque structure were developed while ensuring compliance with the FSAE rules.

After the analysis of each panel, was used CAD design software to model a geometry proposal of the monocoque chassis. In this structure were performed two different analyses, the first being an analysis around the suspension attachment points to validate the strength in the various dynamic loading scenarios, the second being an analysis of torsional stiffness to make a comparison to a space frame chassis.

Using the classical theory of laminates with the different matrices, was possible to predict the behavior of the panel while subjected to a denting force, while varying the plies as well as its location, instead of defining each individual study on the finite element software.

For the reinforcement of the panel, was noticed that placing unidirectional fibers on the direction opposed to the load would increase its overall EI due to the high Young's Modulus present in this type of fiber. Additionally was noticed that the placement of a unidirectional fiber as the second ply instead of right before the core would translate, for the same applied force, into a decrease in the deflection of the panel of around 37% compared to 32%, this happens due to the unidirectional fibers being further from the center line of the laminate, as can be seen by the equations above in the calculus of the matrix $[D_{ij}]$.

For reinforcing the shear capabilities of the different panels, were added more bi-directional fibers with different orientations at 30 or 45 degrees in order to increase the various orientations shear strength.

In the finite element analyses, it could be concluded, that by increasing the core thickness, the distance between the laminate and the neutral line as well as the cross-section of the panel will also increase, which will result in a greater flexural stiffness of the sandwich panel, by the FEA was concluded that the difference by increasing the thickness of the core from 10 to 15 millimeters the EI would increase around 87% whereas from 15 to 20 millimeters the increase would only be around 35%.

In the development of the monocoque geometry it was noted that designing a structure of this complexity takes a lot of time, but also very information from other departments, this is important for the structure to take into account the many loads from the pedal box, steering rack, steering wheel, which are as important as the other points.

By comparing the performance of the two types of chassis, a space frame and a monocoque chassis can be concluded that the level of complexity that is needed in order just to design and develop a monocoque structure is much bigger than designing a tubular chassis.

In terms of torsional stiffness the monocoque will, in most cases, turn out to be superior due to the greater stiffness of the whole panels that make up the structure, while the structure studied was in fact heavier than the tubular chassis from the previous formula student vehicle, due to lack of optimization, it would also be a lot more expensive to build, due to the high pricing of the materials tolls and machining for the molds that it are required through all the manufacturing process, as well as harder and would require a higher attention to detail, in order to avoid surface and structural flaws that could lead into failure, which could compromise the safety of the driver, which is one of the biggest concerns in a motorsport competition.

5.2 FUTURE WORK

For further developments, it is proposed to optimize the monocoque geometry in order, not just to suit the more specific needs of the team, like all the other parts that need to be attached to the monocoque structure, but also to have a better structural performance as it was mentioned above, by reducing the number of edges and making the fillets bigger will not exist such localized spots of stress that weaken the structure.

Due to this analyses being very iteration heavy, is important to use a computer that has greater multitasking capabilities in order to optimize the time spent waiting for the FEA to show results, it is also recommended to use FE software that allows importing the geometry through a solid model in order to preserve as much detail of the original geometry since Ansys can only define the composite materials in surface models.

It can also be developed a more detailed study around the structural adhesives between the core and the laminate as well as between the insert and the honeycomb core, and the many types of insert geometries, materials, and optimization.

One of the most important things in this kind of competition is the validation of the work that has been simulated, through different software crossed into real life, with lab real specimens in order to know how much error exists between the two processes, this will allow defining how much a safety factor needs to be taken into account, as well as, the difference between the two.

The development of a structural composite structure that will suffer from dynamic loads, would also be extremely important, in addition to the static structural analysis, to make a fatigue analysis of the structure, which by creating cyclic loads from various dynamic scenarios with all the loads such as the suspension loads, the loads the pilot applies into the steering wheel, seat, etc...

BIBLIOGRAPHY

[1] European Aluminium. "Lightweighting: a solution to low carbon mobility Making every gram CO2 saving count". In: (2018).

[2] J. N. (Junuthula Narasimha) Reddy and J. N. (Junuthula Narasimha) Reddy. *Mechanics of laminated composite plates and shells : theory and analysis*. CRC Press, 2004, p. 831. ISBN: 9780849315923. URL: https://www.routledge.com/Mechanics-of-Laminated-Composite-Plates-and-Shells-Theory-and-Analysis/Reddy/p/book/9780849315923.

[3] Christian. Decolon. *Analysis of composite structures*. HPS, 2002, p. 336. ISBN: 9781903996621.

[4] Abdul Salam Kaddour and Michael J. Hinton. "1.23 Failure Criteria for Composites". In: (Jan. 2018), pp. 573–600. DOI: 10.1016/B978-0-12-803581-8.10354-6.

[5] R S Sandhu. "AD-756 889 A SURVEY OF FAILURE THEORIES OF ISOTROPIC AND ANISOTROPIC MATERIALS". In: (1972).

[6] R. Hill. "The Theory of Plane Plastic Strain for Anisotropic Metals". In: *Proceedings of the Royal Society of London. Series A, Mathematical and Physical Sciences* 198.1054 (1949), pp. 428–437. ISSN: 00804630. URL: http://www.jstor.org/stable/98277 (visited on 09/27/2022).

[7] Bryan Harris. *Fatigue in Composites: Science and Technology of the Fatigue Response of Fibre-Reinforced Plastics*. Elsevier Ltd, 2003, pp. 1–742. ISBN: 9781855736085. DOI: 10.1533/9781855738577.

[8] *Formula 1 style monocoque - internal structure - F1technical.net*. URL: https://www.f1technical.net/forum/viewtopic.php?t=13148.

[9] *McLaren Racing - Heritage - MP4/1*. URL: https://www.mclaren.com/racing/heritage/cars/1981-formula-1-mclaren-mp4-1/.

[10] Carl Andersson Eurenius, N. Danielsson, Aneesh Khokar, et al. "Analysis of Composite Chassis". In: *undefined* (2013).

[11] Formula Student Team RWTH Aachen. *eace08*. URL: https://www.ecurie-aix.de/en/eace08.

[12] William F. Milliken and Douglas L. Milliken. *Race Car Vehicle Dynamics*. Great Britain: Society of Automotive Engineers Inc., 1996.

[13] Mitchell Hiller. "Design of a Carbon Fiber Composite Monocoque Chassis for a Design of a Carbon Fiber Composite Monocoque Chassis for a Formula Style Vehicle Formula Style Vehicle". In: (2020). URL: https://scholarworks.wmich.edu/honors_theses.

[14] Thomas D. Gillespie. "Fundamentals of Vehicle Dynamics". In: *Fundamentals of Vehicle Dynamics* (Feb. 1992). DOI: 10.4271/R-114.

[15] Society of Automotive Engineers. *Formula SAE, Structural Equivalency Spreadsheet*. Version 2. SAE. International, 2022.

[16] João Eduardo Palma Carpinteiro, Doutor Ricardo José Fontes Portal Mestre Afonso Manuel da Costa de Sousa Leite Júri, Doutor Silvério João Crespo Marques, et al. "INSTITUTO SUPERIOR DE ENGENHARIA DE LISBOA ÁREA DEPARTAMENTAL DE ENGENHARIA MECÂNICA DESENVOLVIMENTO DO SISTEMA DE SUSPENSÃO PARA O CARRO IFS03EE Orientadores: Vogais". In: ().

[17] Calspan Corpuration. "TIRE TESTING INNOVATIONS AT CALSPAN". In: (Sept. 2015).

[18] Lane Thomas Borg. "An Approach to Using Finite Element Models to Predict Suspension Member Loads in a Formula SAE Vehicle". In: (2009).

[19] Society of Automotive Engineers. *Formula SAE, Rules 2022*. Version 2.1. SAE. International, 2022.

[20] Stefano Manzi. "Insert design for sandwich composite monocoque". In: (Apr. 2020).

[21] *188 (52kW — 90Nm) - EMRAX*. EMRAX. URL: https://emrax.com/e-motors/emrax-188/.

[22] *DigitallBattery-Motor-Controller BAMOCAR-D3 for ECCServooMotors ACCInductionnMotors DC-ServooMotors 2 BAMOCARRD3*. UNITEK.

[23] Liam West, Barry Shepherd, Nathaniel Karabon, et al. "Design Report of the High Voltage Battery Pack for Formula SAE Electric". In: (2016).

[24] *XT135/S 250g 3k Tooling Prepreg Carbon 1.25m - Easy Composites*. URL: https://www.easycomposites.eu/xt135-250g-carbon-fibre-tooling-prepreg-surface.

[25] *Vacuum Assisted Resin Infusion Process*. URL: https://www.youtube.com/watch?app=desktop&v=mbrq2fDN8bA.

[26] *XC130 300g Unidirectional Prepreg Carbon Fibre 300mm - Easy Composites*. URL: https://www.easycomposites.eu/xc130-300g-unidirectional-prepreg-carbon-fibre.

[27] *aluNID - High Quality Aluminium Honeycomb*. URL: https://alunid.com/.

[28] *EasyCell75 Closed Cell PVC Foam - Easy Composites*. URL: https://www.easycomposites.eu/easycell75-closed-cell-pvc-foam.

[29] J. Formiga, L. Sousa, and V. Infante. "Numerical and Experimental Analysis of the Suspension Connection Zone of a Formula Student Monocoque Chassis". In: *Procedia Structural Integrity* 17 (Jan. 2019), pp. 886–893. ISSN: 2452-3216. DOI: 10.1016/J.PROSTR.2019.08.118.

[30] Timotei Centea, Mark Anders, Daniel Zebrine, et al. "THE CO-CURE OF HONEYCOMB SANDWICH STRUCTURES: PROCESS PHYSICS AND MANUFACTURING STRATEGIES". In: (2018), pp. 24–28.

[31] Leonard Hamilton, Peter Joyce, Chris Forero, et al. "Production of a composite monocoque frame for a formula SAE racecar". In: *SAE Technical Papers* 2 (2013). ISSN: 26883627. DOI: 10.4271/2013-01-1173.

[32] Sérgio Santos. *Mecânica dos Materiais Compósitos*. IPL, 2020.

[33]   FST Lisboa. *FST09e SES*. Instituto Superior Técnico, 2019.

[34]   FSIPLeiria. *T22 SES*. Politécnico de Leiria, 2022.

[35]   *The Manufacturing Magazine - FST*. URL: https://www.fstlisboa.com/manufacturing-magazines.

APPENDIX

APPENDIX A

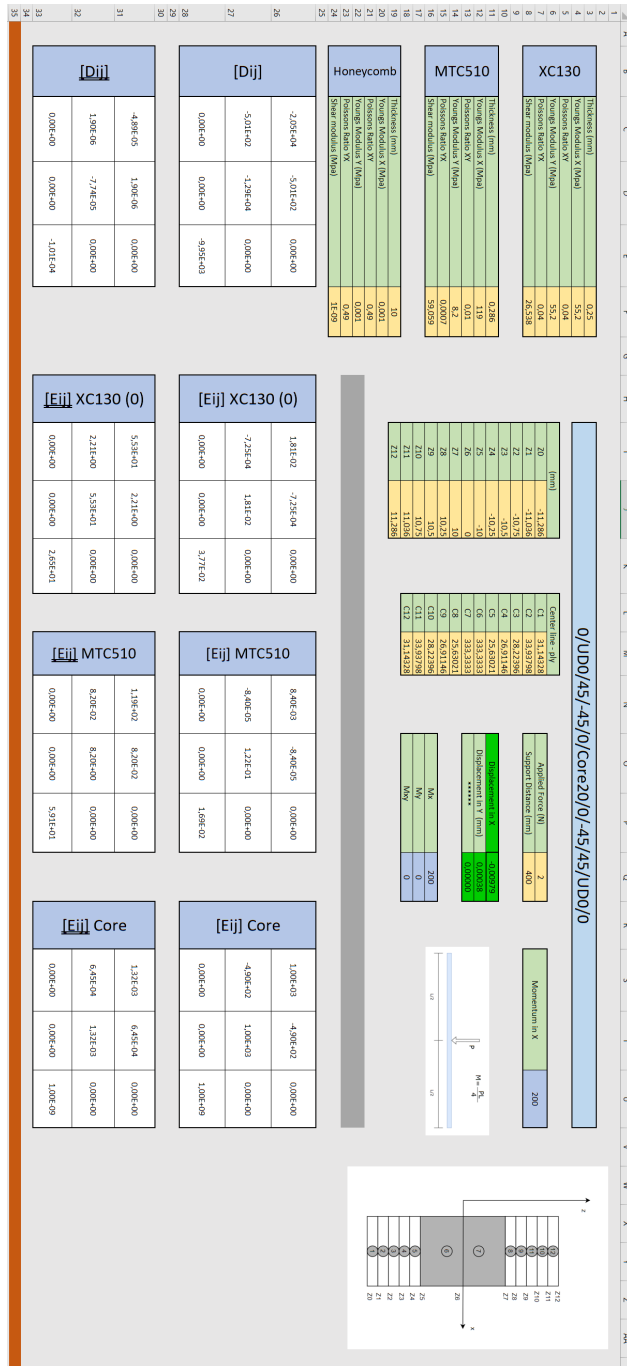Figure 73: Calculus spreadsheet for calculating suspension loads

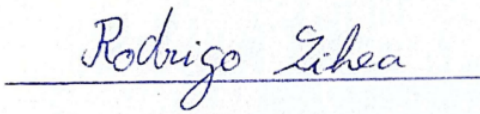Figure 74: Calculus spreadsheet for calculating deflection in bending
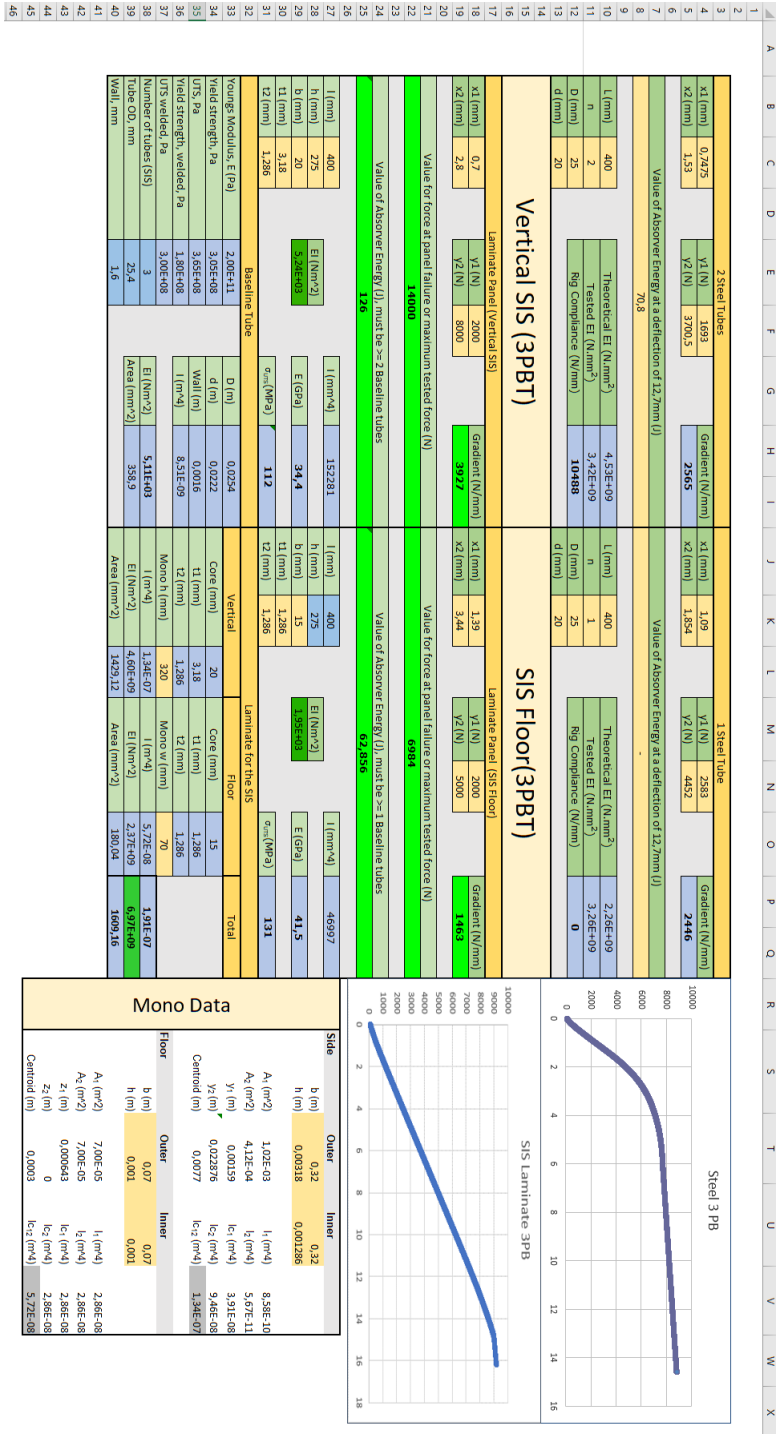
Figure 75: Calculus spreadsheet for calculating panel properties

DECLARATION

Declaro, sob compromisso de honra, que o trabalho apresentado nesta dissertação, com o título *"Chassis development for a Formula Student vehicle using advanced materials"*, é original e foi realizado por Rodrigo Francisco Cerejo da Silva (2202280) sob orientação de Fernando da Conceição Batista (fernando.batista@ipleiria.pt) e co-orientação de Sérgio Pereira dos Santos (ssantos@ipleiria.pt).

Leiria, September 2022